AD-A074 774 STANFORD RESEARCH INST MENLO PARK CALIF F/G 20/14
ANALYSIS OF RADIO-RADAR PROPAGATION CONDITIONS USING SATELLITE---ETC(U)
DEC 75 R H BLACKMER N00228-75-C-2327
UNCLASSIFIED NEPRF-TR-1-76(SRI) NL

1 OF 1
ADA 074774

END
DATE FILMED
11-79
DDC

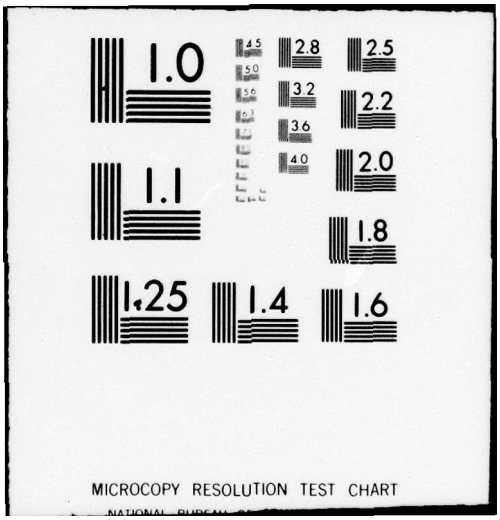
1.0
1.1
1.25
1.4
1.6
1.8
2.0
2.2
2.5
2.8
3.2
3.6
4.0
4.5
5.0
5.6
MICROCOPY RESOLUTION TEST CHART

LEVEL II

NEPRF TR 1-76 (SRI)

Final Report

December 1975

ANALYSIS OF RADIO-RADAR PROPAGATION CONDITIONS USING SATELLITE-VIEWED CLOUD COVER AND RAWINSONDE OBSERVATIONS

By: ROY H. BLACKMER, JR.

Prepared for:

ATMOSPHERIC PHYSICS DEPARTMENT
ENVIRONMENTAL PREDICTION RESEARCH FACILITY
NAVAL POSTGRADUATE SCHOOL
MONTEREY, CALIFORNIA 93940

CONTRACT N00228-75-C-2327

SRI Project 4348

STANFORD RESEARCH INSTITUTE
Menlo Park, California 94025 · U.S.A.

UNCLASSIFIED

SECURITY CLASSIFICATION OF THIS PAGE (When Data Entered)

(19) TR-1-76 (SRI)

REPORT DOCUMENTATION PAGE

READ INSTRUCTIONS BEFORE COMPLETING FORM

1. REPORT NUMBER (12) NEPRF Technical Report 1-76 (SRI)

2. GOVT ACCESSION NO.

3. RECIPIENT'S CATALOG NUMBER

4. TITLE (and Subtitle)

(6) Analysis of Radio-Radar Propagation Conditions Using Satellite-Viewed Cloud Cover and Rawinsonde Observations

5. TYPE OF REPORT & PERIOD COVERED

(9) Final Report, 12 Jun [redacted] - 12 Oct [redacted] 75,

6. PERFORMING ORG. REPORT NUMBER

SRI Project 4348

7. AUTHOR(s)

(10) Roy H. Blackmer, Jr.

8. CONTRACT OR GRANT NUMBER(s)

(15) Contract N00228-75-C-2327

9. PERFORMING ORGANIZATION NAME AND ADDRESS

Stanford Research Institute
333 Ravenswood Avenue
Menlo Park, California 94025

332 500

10. PROGRAM ELEMENT, PROJECT, TASK AREA & WORK UNIT NUMBERS

11. CONTROLLING OFFICE NAME AND ADDRESS

(11) Commander, Naval Air Systems Command
Department of the Navy
Washington, D.C. 20361

12. REPORT DATE: Dec [redacted] 75

13. NO. OF PAGES: 62

14. MONITORING AGENCY NAME & ADDRESS (if diff. from Controlling Office)

Naval Environmental Prediction Research Facility
Monterey, CA 93940

15. SECURITY CLASS. (of this report)

Unclassified

15a. DECLASSIFICATION/DOWNGRADING SCHEDULE

16. DISTRIBUTION STATEMENT (of this report)

Approved for Public Release; distribution unlimited.

(12) 56

17. DISTRIBUTION STATEMENT (of the abstract entered in Block 20, if different from report)

18. SUPPLEMENTARY NOTES

19. KEY WORDS (Continue on reverse side if necessary and identify by block number)

Radio-Radar Propagation
Anomalous Propagation
Refractivity Gradients
Rawinsonde Observations
Satellite-Viewed Cloud Cover

20. ABSTRACT (Continue on reverse side if necessary and identify by block number)

The purpose of this study was to investigate how well the type and variability of satellite-viewed cloud cover may be used to describe the occurrence and variability of anomalous propagation conditions over areas of various sizes. In the investigation six cases were chosen for study covering periods when high received signal levels on the Berlin-Bocksberg-Breistsol tropospheric-scatter communication links indicated the probable occurrence of anomalous propagation. Rawinsonde data over an extended area

DD FORM 1 JAN 73 1473

EDITION OF 1 NOV 65 IS OBSOLETE

UNCLASSIFIED

SECURITY CLASSIFICATION OF THIS PAGE (When Data Entered)

332,500

19. KEY WORDS (Continued)

20 ABSTRACT (Continued)

surrounding the tropospheric scatter links were processed to compute refractivity gradients between the surface and the 700-mb level. These refractivity gradients were plotted on DMSP satellite photographs that showed the cloud cover (or its absence) over the network of rawinsonde stations.

Comparison of the cloud photographs and superimposed refractivity gradients showed considerable variation in height and magnitude of large negative refractivity gradients at adjacent stations even though the stations appeared to have similar cloud cover, or clear skies. The major reason for the variability in refractivity gradients at adjacent stations is considered to be the inadequacy of the rawinsonde data. In particular, the small number of data points in the rawinsondes taken at some of the stations did not describe the atmospheric structure in sufficient detail to define superrefractive or trapping gradients that may have existed over the stations.

Because of the limitations of the rawinsonde data, it was not possible to conclusively show that satellite-viewed cloud cover is a valuable operational indicator of anomalous propagation conditions. In five of the six cases, refractivity gradients of superrefractive or trapping magnitudes were most frequent in clear or partly cloudy areas although the magnitudes and heights of large negative gradients were often quite different at adjacent stations.

None of the cases had widespread multilevel clouds. The only case in which there was widespread, relatively uniform, cloud cover was one in which widespread fog and low clouds occurred beneath a strong low-level inversion and all rawinsonde data in the area showed very large negative refractivity gradients. In this case the satellite observed cloud cover could be used to infer the presence of similar large gradients, and anomalous propagation, throughout the entire area where the satellite photographs showed this clearly characteristic cloud cover.

CONTENTS

LIST OF ILLUSTRATIONS v

LIST OF TABLES ix

I INTRODUCTION 1

II DATA AND ANALYSIS TECHNIQUES 3

A. Data 3

B. Analysis Techniques 6

III CASE STUDIES 9

A. Selection of Cases 9

B. 1200 GMT 1 October to 1200 GMT 2 October 1973 11

C. 1200 GMT 5 October to 1200 GMT 7 October 1973 13

D. 0000 GMT 18 November to 1200 GMT 20 November 1973 19

E. 0000 GMT 9 December to 1200 GMT 12 December 1973 20

F. 0000 GMT 20 January to 1200 GMT 22 January 1974 26

G. 0000 GMT 12 February to 1200 GMT 17 February 1974 36

IV DISCUSSION OF RESULTS 43

V CONCLUSIONS 49

REFERENCES 51

ILLUSTRATIONS

Figure 1 Rawinsonde Station Network and Berlin (BLN) - Bocksberg (BBG) - Breitsol (BTL) Tropospheric Scatter Links 5

Figure 2 Hourly Received Signal Levels During Indicated Periods Between Breitsol (BTL) and Bocksberg (BBG) and Between Berlin (BLN) and Bocksberg 10

Figure 3 Height of Base (km) and Thickness (meters) of Layers with (S) or Trapping (T) N-Gradients on 1 and 2 October 1973 12

Figure 4 Cloud Cover and Refractivity Gradients, 2 October 1973 14

Figure 5 Height of Base (km) and Thickness (meters) of Layers with Superrefractive (S) or Trapping (T) N-Gradients 5 to 7 October 1973 16

Figure 6 Cloud Cover and Refractivity Gradients, 6 October 1973 17

Figure 7 Cloud Cover and Refractivity Gradients, 7 October 1973 18

ILLUSTRATIONS (continued)

Figure 8 Height of Base (km) and Thickness (meters) of Layers with Superrefractive (S) or Trapping (T) N-Gradients 18 to 20 November 1973 21

Figure 9 Cloud Cover and Refractivity Gradients, 19 November 1973 22

Figure 10 Height of Base (km) and Thickness (meters) of Layers with Superrefractive (S) or Trapping (T) N-Gradients 9 to 12 December 1973 24

Figure 11 Cloud Cover and Refractivity Gradients, 9 December 1973 25

Figure 12 Cloud Cover and Refractivity Gradients, 11 December 1973 27

Figure 13 Height of Base (km) and Thickness (meters) of Layers with Superrefractive (S) or Trapping (T) N-Gradients 20 to 22 January 1974 29

Figure 14 Time Sections of Refractivity Gradients (N-Units/km) at Essen and Meiningen 20 to 23 January 1974 31

Figure 15 Cross Sections of Refractivity Gradients (N-Units/km) along the Breitsol (BTL) Bocksberg (BBG) Berlin (BLN) Tropospheric Scatter Links, 21 to 23 January 1974 . . 32

ILLUSTRATIONS (concluded)

Figure 16 Cloud Cover and Refractivity Gradients, 19 January 1974 34

Figure 17 Cloud Cover and Refractivity Gradients, 21 January 1974 35

Figure 18 Height of Base (km) and Thickness (meters) of Layers with Superrefractive (S) or Trapping (T) N-Gradients 14 to 17 February 1974 38

Figure 19 Cloud Cover and Refractivity Gradients, 15 February 1974 39

Figure 20 Cloud Cover and Refractivity Gradients, 16 February 1974 40

TABLES

Table 1 Frequency of Superrefractive or Trapping Gradients at Various Stations 45

Table 2 Comparison of Number of Data Points in Rawinsonde Ascents at Two Stations During Periods Studied . . 46

I INTRODUCTION

This report describes the results of a study comparing refractivity gradients derived from rawinsonde data with the type and distribution of satellite-viewed cloud cover. The objective of the study was to determine the extent to which the type and variability of satellite-viewed cloud cover may be used to indicate the occurrence and variability of anomalous propagation conditions over areas of various sizes.

The use of cloud cover to describe the vertical distribution of temperature and moisture was investigated by Blackmer et al. (1968).* They compared cloud cover, classified in nine categories according to the type, height, and band location, with departures of vertical temperature and moisture profiles from seasonal normals. Their results showed that given classes of cloud cover were superior to climatological means in describing temperature and moisture profiles. Although the results of this study were not applied to the problem of estimating propagation conditions from cloud cover, other studies have related cloud cover to propagation conditions. Serebreny and Blackmer (1974) and Blackmer (1974) compared received signal levels on tropospheric scatter communication links with the type and appearance of cloud cover (as photographed from meteorological satellites) over the links. Data from two areas were studied.

---

* References are listed at the end of the report.

The first area was off the coast of China where, during the winter, outbreaks of very cold air from the Asian mainland move over the much warmer water of the western Pacific Ocean producing substantial instability. Invariably, daily median received signal levels decreased when these cold outbreaks occurred. The cloud cover over the links had a distinctive cellular appearance during these cold outbreaks and thus could serve as an indicator of poor propagation conditions. However, the only data available were daily medians and since these were not felt to be optimum for comparison with cloud photographs, it was arranged to collect more detailed data on European tropospheric scatter links.

The second area that was studied was in Europe, where radio propagation data were in the form of continuous strip chart recordings of received signal levels. Various analyses were made of these data with the results that the type of cloud cover appeared to supply useful information on signal levels to be expected over the links. In this present study many of the data collected for the second study mentioned above (Blackmer, 1974) are being used. The basic difference between the two studies is that in the previous study emphasis was on the comparison of cloud cover with signal levels over tropospheric scatter links on an overall basis. In the current study emphasis is on comparison of cloud cover and refractivity gradients in situations where anomalous propagation was occurring on the tropospheric scatter links. The refractivity gradients were computed from rawinsonde observations both in the immediate vicinity of the links at the time of occurrence of anomalous propagation and at various distances from the links before and after the period of anomalous propagation.

Section II of this report describes the available data and analysis techniques, Section III contains a series of case studies, Section IV discusses the results of the case studies, and Section V presents the conclusions.

II DATA AND ANALYSIS TECHNIQUES

A. Data

1. Satellite Photographs

The cloud cover photographs used in this study were from satellites 5528 and 7529 of the U.S. Air Force Weather Service's Data Acquisition and Processing Program (DAPP). As described by Meyer (1973) and Blankenship and Savage (1974), the DAPP satellites operate from an altitute of 450 miles* in sun synchronomous orbits. Two satellites are normally maintained in orbit, one in a noon-midnight orbit, and the other in an early morning-evening orbit. The imagery data collected, by a four-channel linescan radiometer, consist of visual (0.4 to 1.14 um) and infrared (8 to 13 um) spectral types. Each spectral type is divided into two resolution categories. These are two-mile or 1/3 mile resolution at the subpoint.

A capability exists to threshold the data at three selected temperatures to give four shades of grey corresponding to temperature intervals bracketed by the selected temperatures. The resulting four grey shade photographs supply information on relative heights of various areas of cloud cover. Examples of the various photographs will be shown in Section III.

---

* Nautical miles are used throughout this report.

2. Rawinsonde Data

The primary rawinsonde data used in this study were computer printouts of data for selected stations in western Europe. Values of pressure, temperature, and dew-point depression at mandatory and significant levels from the surface to the 700-mb level were placed on punched cards for computation of refractivity gradients.

A second source of rawinsonde data was plotted soundings transmitted via facsimile to European weather stations. A sheet of facsimile paper approximately 19 x 24 inches contained four panels, each with three soundings. Three such sheets were transmitted twice daily, giving a total of 36 soundings at each observation time. Some of these soundings were outside the area of interest and a number of them were duplications of the data contained in the computer listings. They were, however, a useful source of information for examining the shape of the sounding.

Figure 1 shows the distribution of stations from which these two types of rawinsonde data were available and also shows the location of the Berlin to Bocksberg and Bocksberg to Breitsol tropospheric scatter links.

3. Supporting Data

In addition to the rawinsonde data on facsimile charts described above, a number of other products transmitted over the facsimile circuit were available. These included three-hourly surface charts, six-hourly surface charts, six-hourly upper air data at selected levels, and 12-hourly upper air charts. These products were useful for examining the synoptic situation and the three-hourly surface charts were especially useful since they contained detailed observations of cloud cover and present weather. These observations aided in the interpretation of cloud types and in determining the presence of low

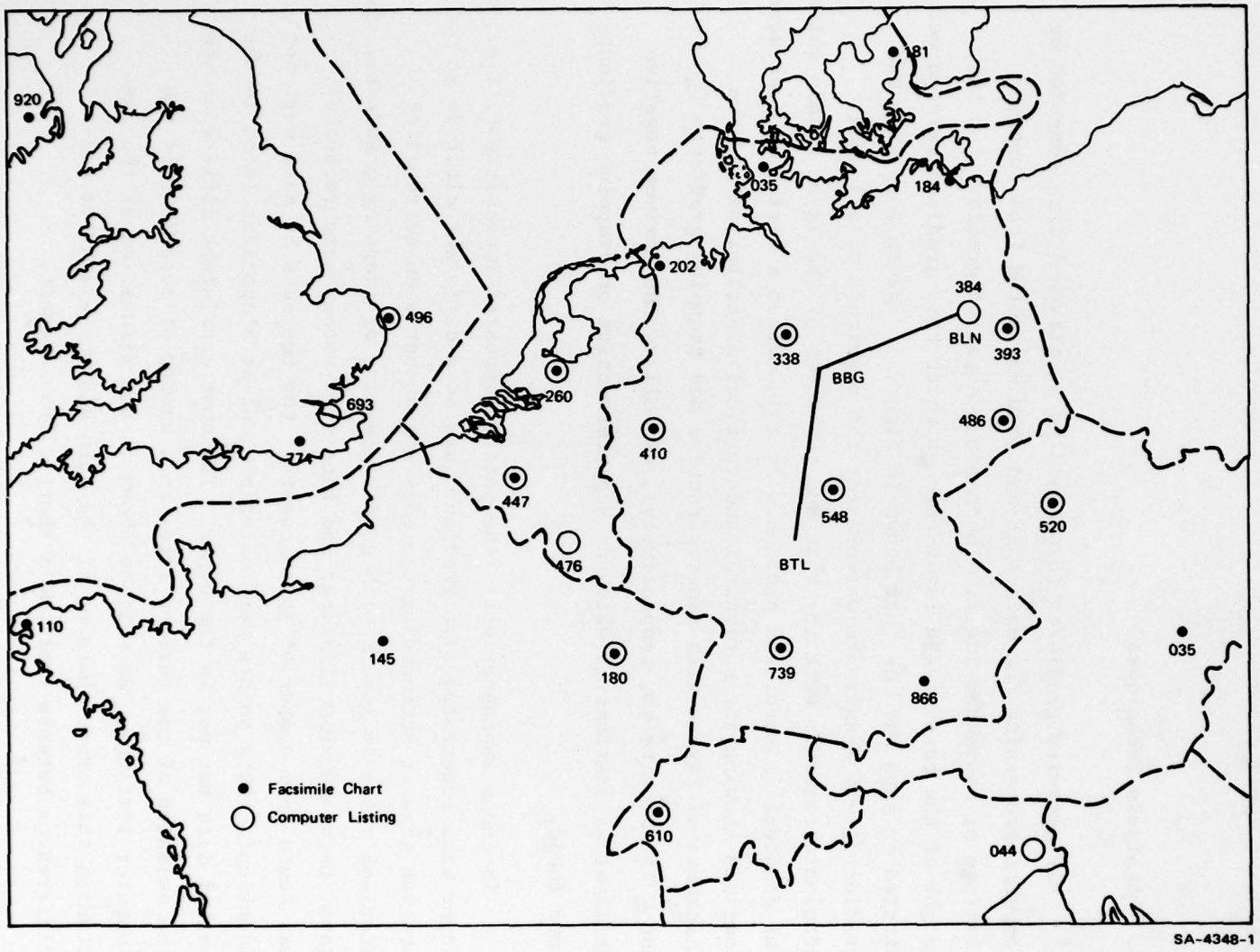

FIGURE 1 RAWINSONDE STATION NETWORK AND BERLIN (BLN)—BOCKSBERG (BBG)—BREITSOL (BTL) TROPOSPHERIC SCATTER LINKS

clouds or fog in situations where the satellite photographs showed extensive upper clouds.

B. Analysis Techniques

Refractivity gradients (expressed in N-units/km) were computed by computer processing the data that had been extracted from computer listings of rawinsonde data. The maximum negative gradient and the height of the base of the layer through which this gradient existed were plotted on maps such as that shown in Figure 1. Where more than one gradient $\leq$ -79 N-units/km was present the magnitude of all such gradients together with the base and thickness of the layer within which the gradient existed, was plotted. By this method a series of maps were compiled showing the horizontal and vertical distribution and the thickness of layers with superrefractive and trapping gradients ($\leq$ -79 and $\leq$ 157 N-units/km, respectively), as well as the maximum negative gradient at stations at which no superrefractive or trapping gradients were found.

In those instances where the pattern appeared inconsistent, i.e., a layer with superrefractive gradients was at a different altitude at one station than at surrounding stations, or absent when surrounding stations all show layers with superrefractive or trapping gradients, the data, both computer listings and facsimile raobs, were rechecked. It was found in a number of instances that the two sets of data were not identical. Data points were often present at a specific level in one set of data but not in the other. The most consistent difference was the omission of the surface level on a number of occasions in the computer listings. As will be shown in the discussion of the case studies this cross checking of the data did not eliminate all the differences between stations a short distance apart.

After rechecking the data, the height of the base and thickness of layers with superrefractive and trapping gradients were summarized on one map for each case study. In addition, the data on maps for specific times were plotted on overlays superimposed on the satellite photographs closest to the time of the rawinsonde observations, for comparison of refractivity gradients with the type and distribution of cloud cover.

In the evaluation of the type and distribution of cloud cover, four grey shade IR photographs were used whenever possible to obtain information on the probable vertical extent of the cloud cover.

Additional analysis consisted of an examination of six-hourly surface charts to obtain a brief description of the general synoptic situation and a quick look at both the satellite photographs and the three-hourly surface charts for a brief description of the major features of the cloud cover.

III CASE STUDIES

A. Selection of Cases

In a previous study (Blackmer, 1974), a series of plots of signal level at hourly intervals over the tropospheric scatter links between Breitsol (BTL) and Bocksberg (BBG), and Berlin (BLN) and Bocksberg were made for two-week periods in October, November, and December 1974. Portions of these plots, shown in Figure 2, were examined and several dates and times selected for analysis. The basis of the selection was (1) the occurrence of high signal levels, indicative of superrefraction or trapping, on either the BLN to BBG or BTL to BBG tropospheric-scatter communication links, and (2) the availability of rawinsonde data. Using these criteria, the periods initially selected for study were:

1200 GMT 1 October to 1200 GMT 2 October 1973
1200 GMT 5 October to 1200 GMT 7 October 1973
0000 GMT 18 November to 1200 GMT 20 November 1973
0000 GMT 9 December to 1200 GMT 12 December 1973
0000 GMT 20 January to 1200 GMT 22 January 1974
0000 GMT 12 February to 1200 GMT 17 February 1974

The detailed treatment of these various cases is discussed in the following sections of this report.

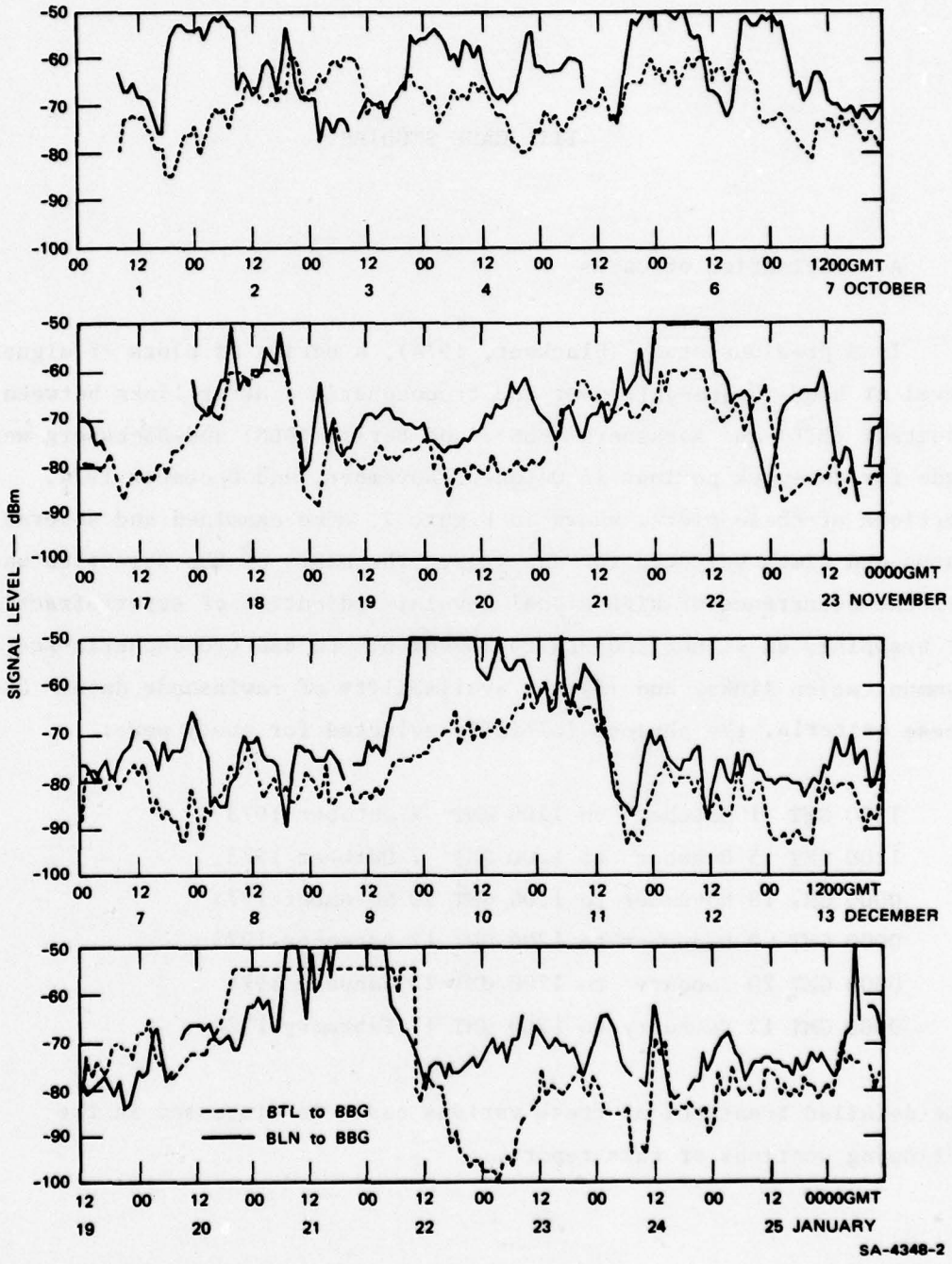

FIGURE 2 HOURLY RECEIVED SIGNAL LEVELS DURING INDICATED PERIODS BETWEEN BREITSOL (BTL) AND BOCKSBERG (BBG) AND BETWEEN BERLIN (BLN) AND BOCKSBERG

B. 1200 GMT 1 October to 1200 GMT 2 October 1973

1. Synoptic Situation

During this period, there was a large anticyclone in the eastern Atlantic that moved northeastward to Ireland from an initial position 300 miles southwest of Ireland. A ridge of high pressure extending eastward from this anticyclone covered much of western Europe.

2. Cloud Cover

Cloud cover over the area of interest was generally scattered cumulus and stratocumulus at 1200 GMT on the 1st. At 0000 GMT on the 2nd these small cumulus, caused by solar heating, had dissipated and skies were generally clear. By 1200 GMT 2 October, middle and upper clouds in advance of a warm front in the Western Mediterranean were moving into southwestern Europe.

3. Refractivity gradients

During the period, refractivity gradients of superrefractive or trapping magnitude were rather randomly distributed. Figure 3 shows the height (in km above sea level) and thickness (in meters) of layers with refractivity gradients of superrefractive (S) or trapping (T) magnitude. The figure contains data for three different times and inspection of the figure shows that at any given time some stations had surface-based superrefractive layers, some had elevated superrefractive layers, while others had no such layers. There were no gradients of trapping magnitude during the three times examined; the maximum gradient was -121 N-units/km at station 338 at 0000 GMT on the 2nd.

Figure 3 shows some persistence of a given condition at various stations. For example, stations 496 and 410 had layers with superrefractive gradients above 1 km at all three times, stations 447,

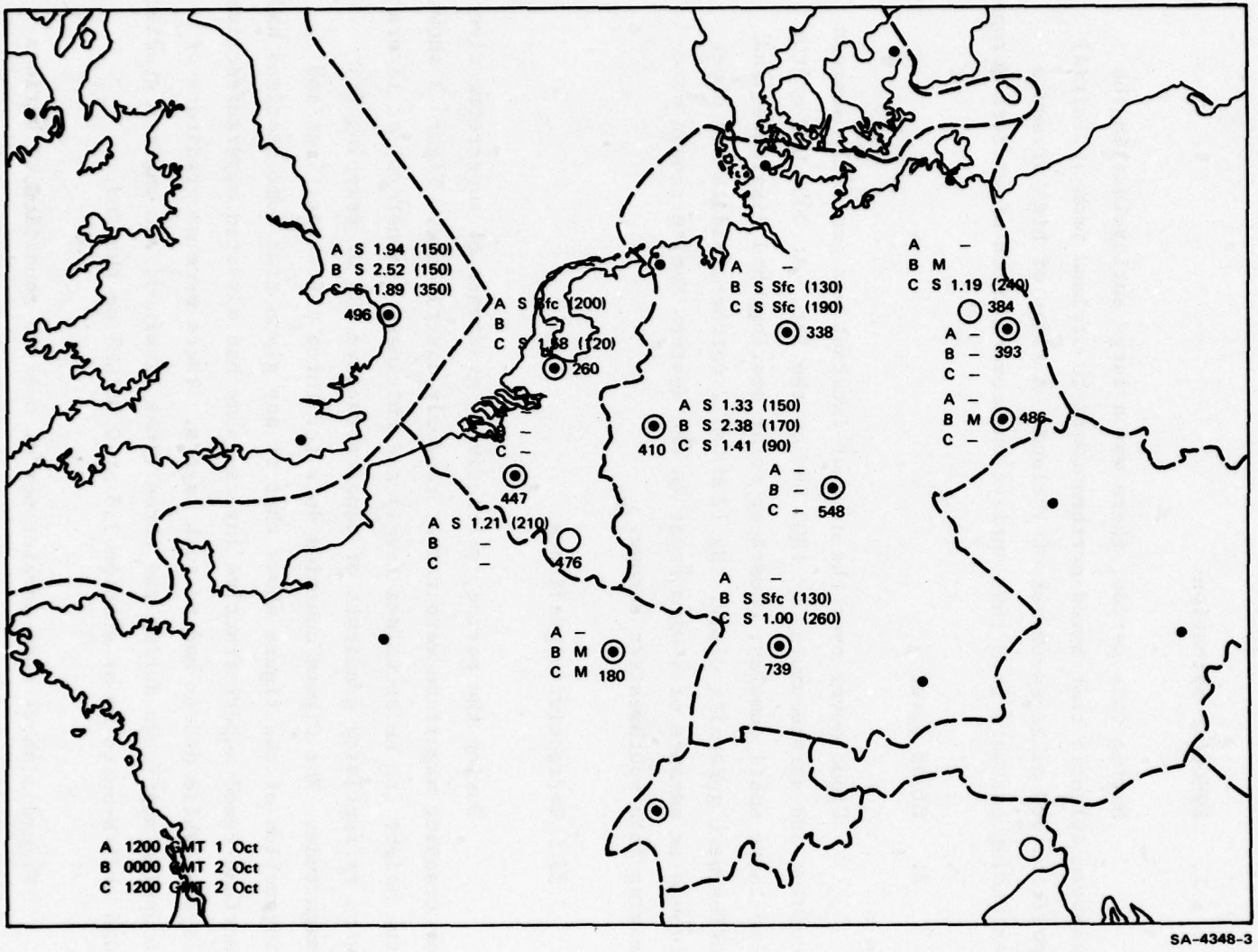

FIGURE 3 HEIGHT OF BASE (KM) AND THICKNESS (METERS) OF LAYERS WITH SUPERREFRACTIVE (S) OR TRAPPING (T) N-GRADIENTS ON 1 AND 2 OCTOBER 1973

548, and 393 consistently had no layers with superrefractive gradients, and the only two layers with superrefractive gradients at station 338 were based at the surface. Station 260, about halfway between stations 496 and 410 which both have layers with superrefractive gradients aloft all three times, had a superrefractive gradient based at the surface, no superrefractive gradient, and a superrefractive gradient aloft.

Figure 4 contains cloud photographs at 0127 GMT 2 October, with an overlay showing the maximum negative refractivity gradients at the stations from which computer listings of rawinsonde data were available at 0000 GMT 2 October. Comparisons of the cloud cover and these gradients shows that although the area appears mostly clear there is considerable variability in the height and magnitudes of the maximum negative refractivity gradients. This variability in refractivity gradients was also evident in the comparison of refractivity gradients and cloud cover at 1200 GMT 1 October and 1200 GMT 2 October.

C. 1200 GMT 5 October to 1200 GMT 7 October 1973

1. Synoptic Situation

At the start of this period there was a filling low pressure center 200 miles south of Ireland and a high pressure area over southern Poland. This resulted in a very weak southerly flow over eastern Europe. During the period, the two pressure systems mowed slowly eastward. The low pressure center filled and a second small high pressure area moved into western France.

2. Cloud Cover

During most of the period there was no cloud cover in the vicinity of stations for which refractivity gradients were available.

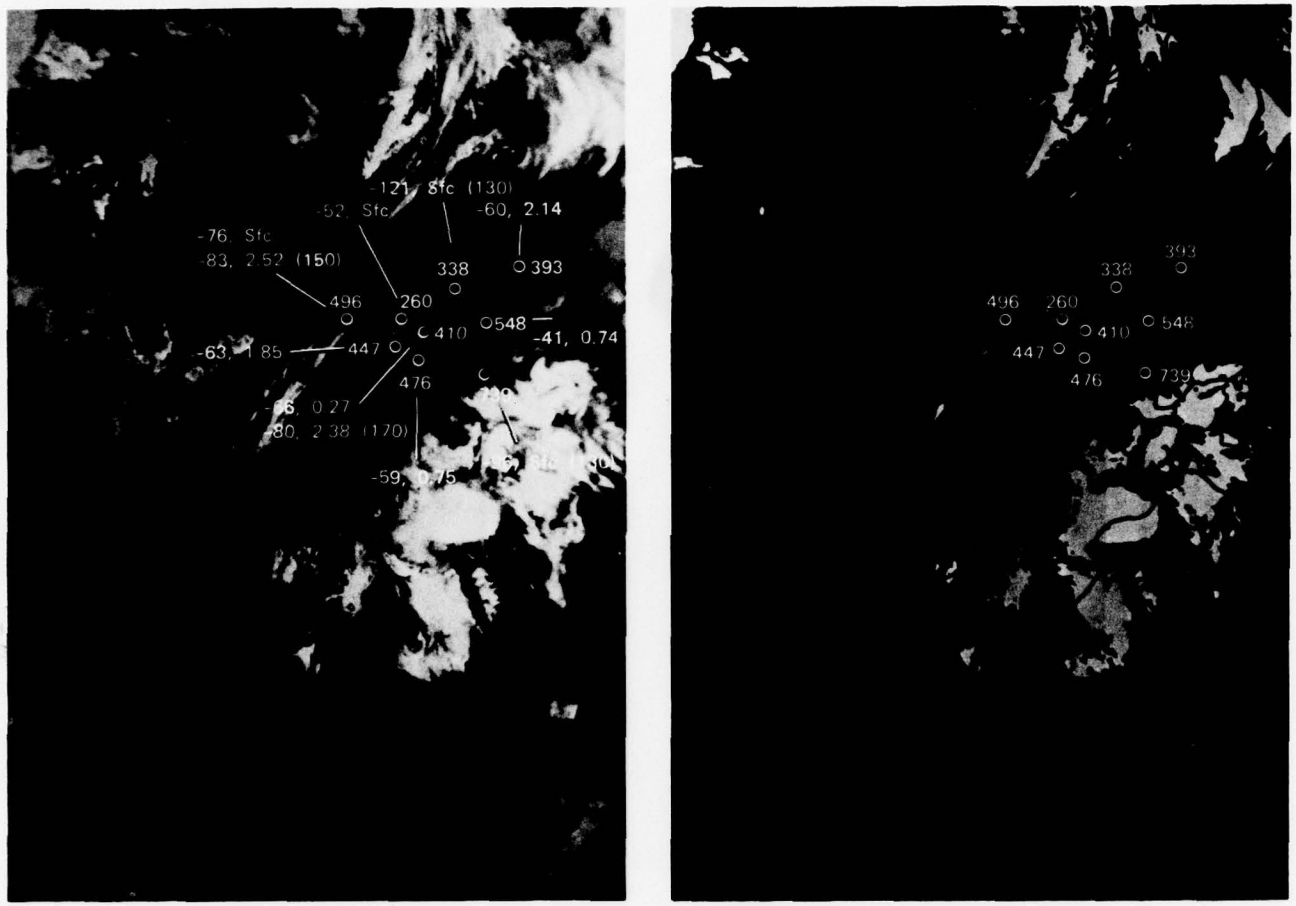

SA-4348-4

16 GREY SHADE IR

4 GREY SHADE IR

FIGURE 4 CLOUD COVER AND REFRACTIVITY GRADIENTS, 2 OCTOBER 1973

It was only toward the end of the period that cloudiness associated with a weak front moved into the western portion of the area.

3. Refractivity Gradients

Many of the rawinsonde ascents during the period contained multiple layers with superrefractive or trapping gradients between the surface and the 700-mb level. These layers varied in thickness from 10 meters to 560 meters. Temperature inversions were generally small and most of them were close to the surface.

Figure 5 shows the distribution of layers with superrefractive and trapping gradients during the period studied. Only two stations (496 and 338) had layers with superrefractive and trapping gradients at all five times examined. As the figure shows, at any given time there was a general lack of continuity between adjacent stations.

Figure 6 shows cloud cover at 0028 GMT 6 October and refractivity gradients computed from rawinsonde data taken about 28 minutes earlier. Data on the overlay show that the majority of the stations have layers with superrefractive and trapping gradients based at the surface and many stations have additional layers aloft. Only one station (260) does not show a layer with superrefractive or trapping gradients. The cloud cover at this latter station is not significantly different from that at the others. (The two bright circular clouds at the left of the photographs are developing thunderstorms.)

Figure 7 shows cloud cover at 0014 GMT and refractivity gradients at 0000 GMT on 7 October. At this time there are multiple layers with superrefractive gradients at the surface and aloft both in the cloudy and clear areas. Two stations (447 and 548), however, do not have gradients of superrefractive magnitude. Station 548 appears to be in the same clear area as station 338 while the cloud cover over

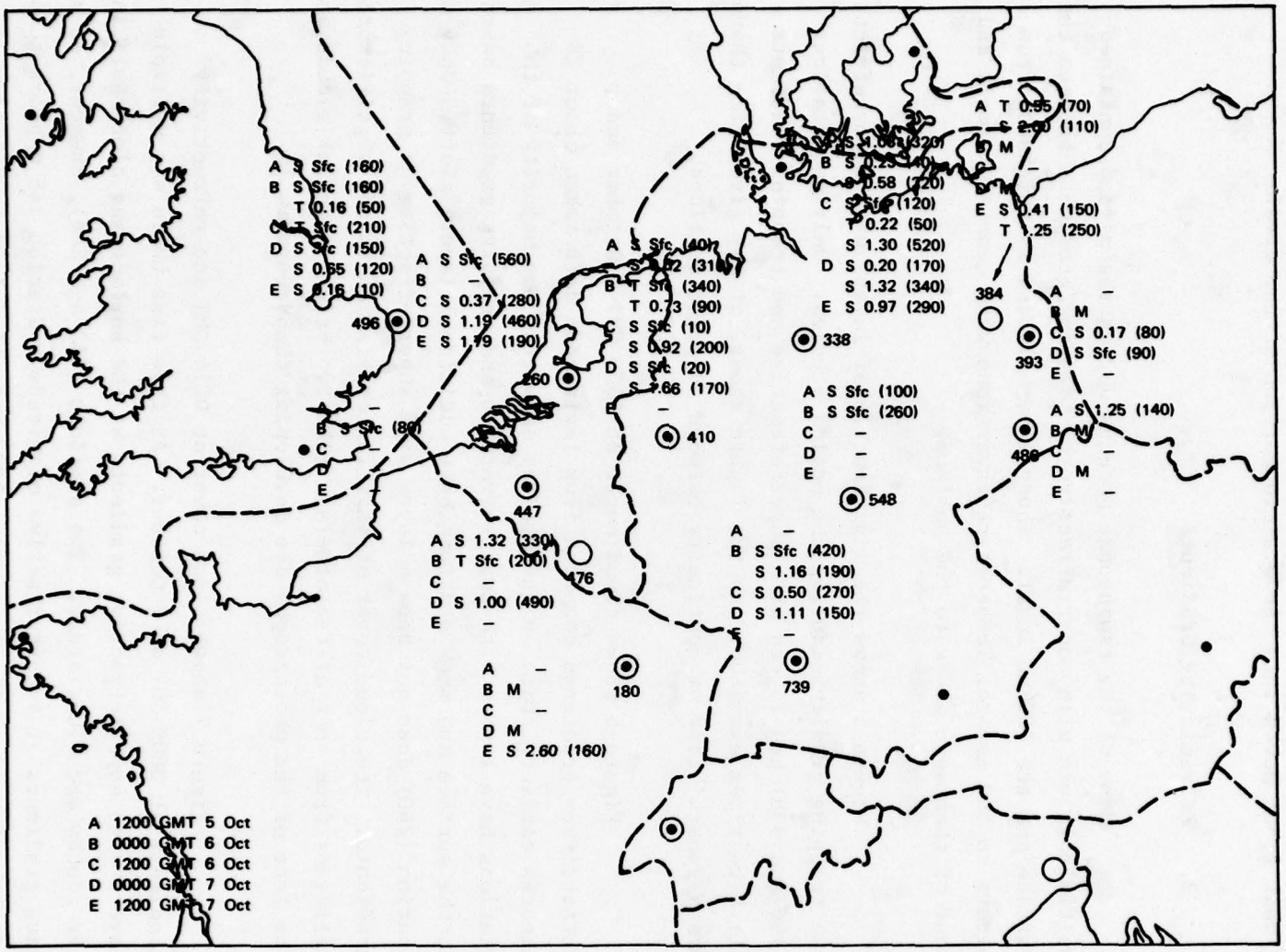

FIGURE 5 HEIGHT OF BASE (KM) AND THICKNESS (METERS) OF LAYERS WITH SUPERREFRACTIVE (S) OR TRAPPING (T) N-GRADIENTS 5 TO 7 OCTOBER 1973

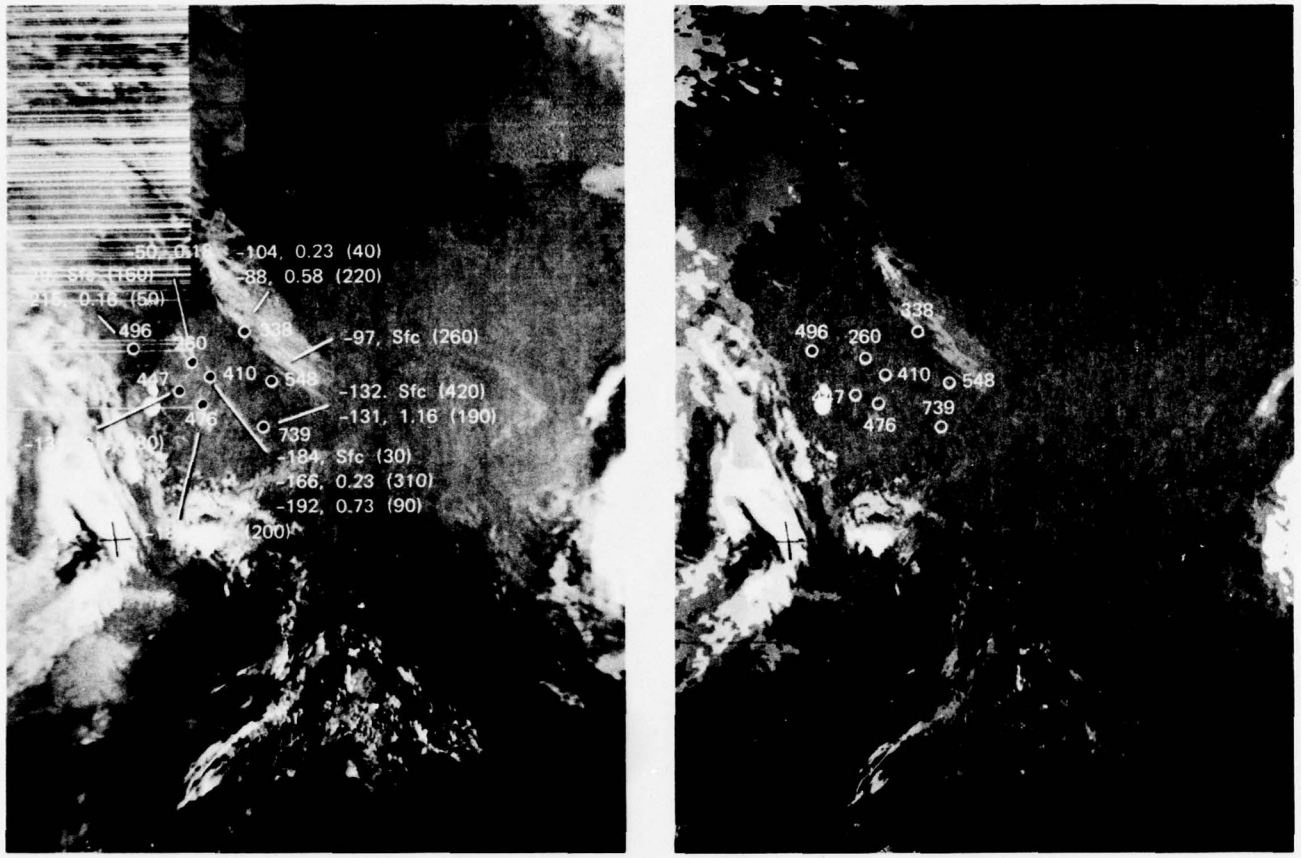

SA-4348-6

16 GREY SHADE IR

4 GREY SHADE IR

FIGURE 6 CLOUD COVER AND REFRACTIVITY GRADIENTS, 6 OCTOBER 1973

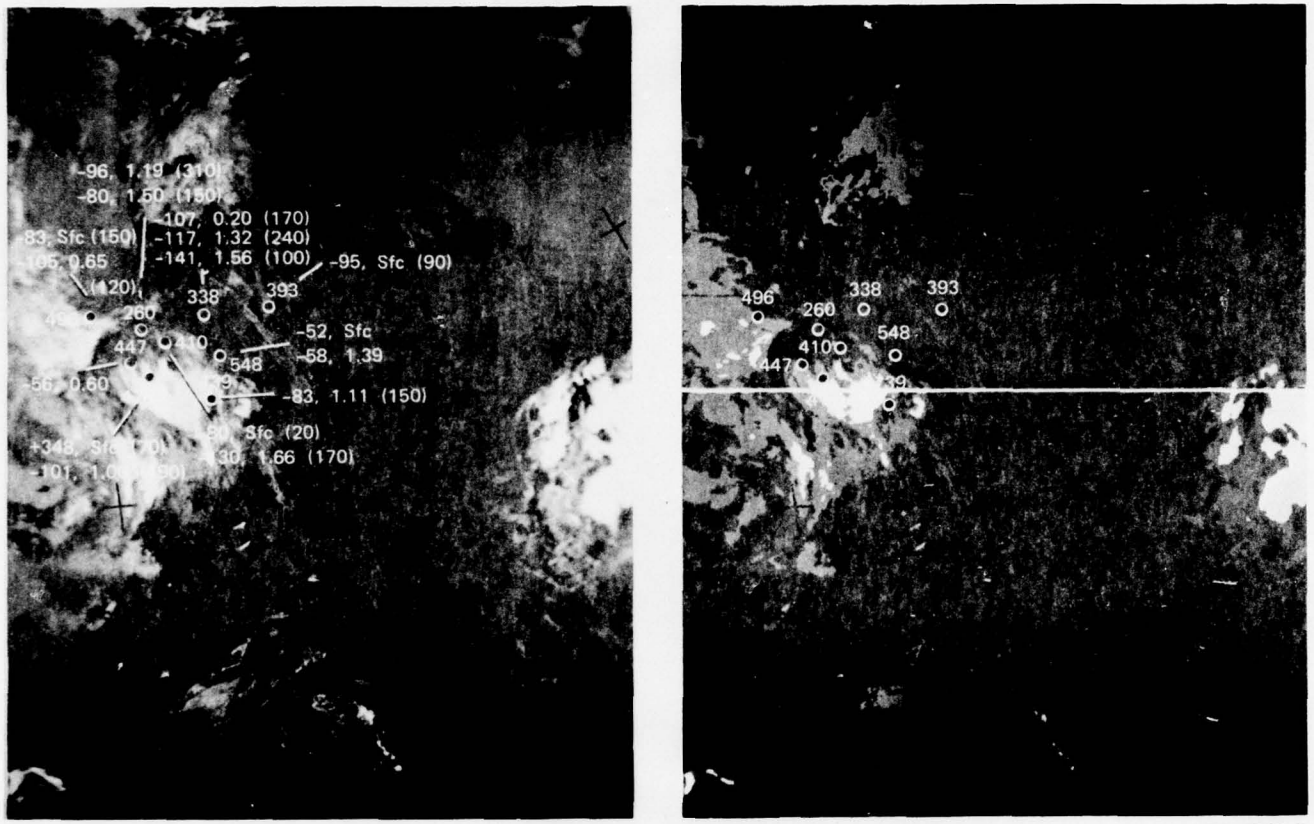

16 GREY SHADE IR

4 GREY SHADE IR

SA-4348-7

FIGURE 7 CLOUD COVER AND REFRACTIVITY GRADIENTS, 7 OCTOBER 1973

stations 447 and 410 appears similar. The whitest cloud on the right photograph in Figure 7 is colder than -19C which would locate it above the 500-mb level.

The comparisons of cloud cover and refractivity gradients at the other three times showed a similar mixture of stations with layers of superrefractive and trapping gradients at the surface and aloft surrounding stations without such layers. There appeared to be no significant differences in the cloud cover (or its absence) over the stations with or without layers with superrefractive and trapping gradients.

D. 0000 GMT 18 November to 1200 GMT 20 November 1973

1. Synoptic Situation

During the period a high pressure area moved eastward from an initial location over central Germany. A deepening low pressure center moved eastward just north of Scotland and its cold front moved southeastward through the area of interest during the 19th. A high pressure area moving southeastward behind the low pressure center extended into the area of interest on the 20th.

2. Cloud Cover

At the start of the period much of the area was clear although there was some cirrus and middle cloud in the northwest portion of the area of interest. The most extensive cloud cover was with the frontal band which passed through the area on the 19th. Cloud cover behind the front consisted of towering cumulus, with some showery precipitation, and stratocumulus.

3. Refractivity Gradients

Figure 8 shows the distribution of layers with superrefractive and trapping gradients during the period. The figure shows that the distribution is rather random. Station 260 had layers with superrefractive and trapping gradients at all six times examined while station 447, fairly close to 260, had no layers with superrefractive or trapping gradients. Station 393 also had no layers with superrefractive or trapping gradients during the period while station 384, just to the northwest, had superrefractive gradients at two of the three times with data. The majority of the layers with superrefractive and trapping gradients had bases above the 1 km level but the layers do not appear to have spatial continuity.

Figure 9 shows cloud cover at 0139 GMT 19 November and refractivity gradients at 0000 GMT 19 November. The largest negative refractivity gradient on this figure is at station 260 in the frontal band. Two stations ahead of the band have layers with superrefractive gradients: at the surface at station 476, and at 1.53 km at station 548. A third station (739), well ahead of the band, has a surface based gradient of -76 N-units/km which is close to superrefractive magnitude. At other times during the period covered by this case study, the occurrence of layers with superrefractive and trapping gradients did not appear to correspond to the type and distribution of cloud cover or the distribution of cloud free areas.

E. 0000 GMT 9 December to 1200 GMT 12 December 1973

1. Synoptic Situation

At the start of the period there was a low pressure center located over eastern Poland and a high pressure area centered 600 miles west of the northwest tip of Spain. The high pressure area moved

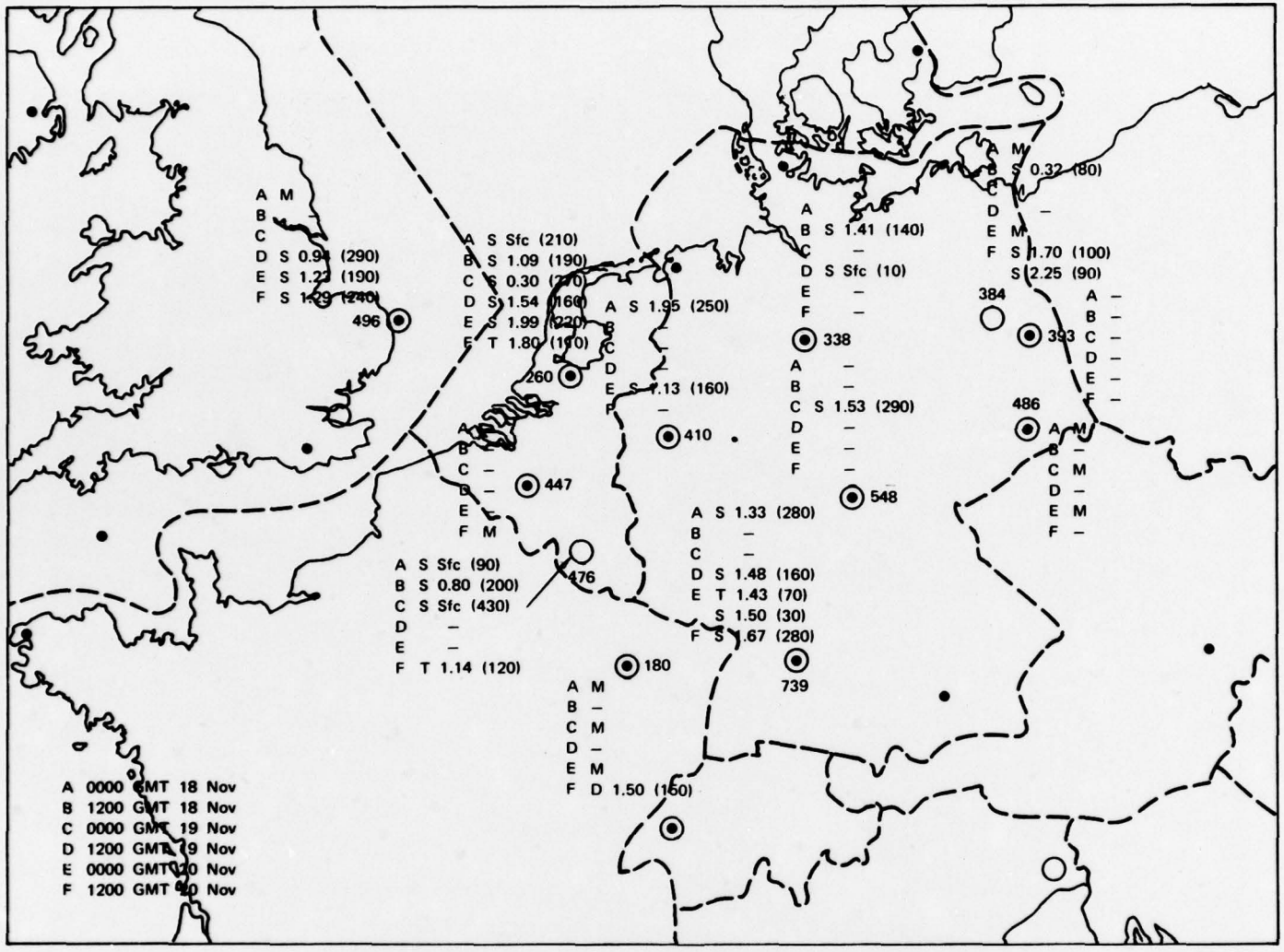

SA-4348-8

FIGURE 8 HEIGHT OF BASE (KM) AND THICKNESS (METERS) OF LAYERS WITH SUPERREFRACTIVE (S) OR TRAPPING (T) N-GRADIENTS 18 TO 20 NOVEMBER 1973

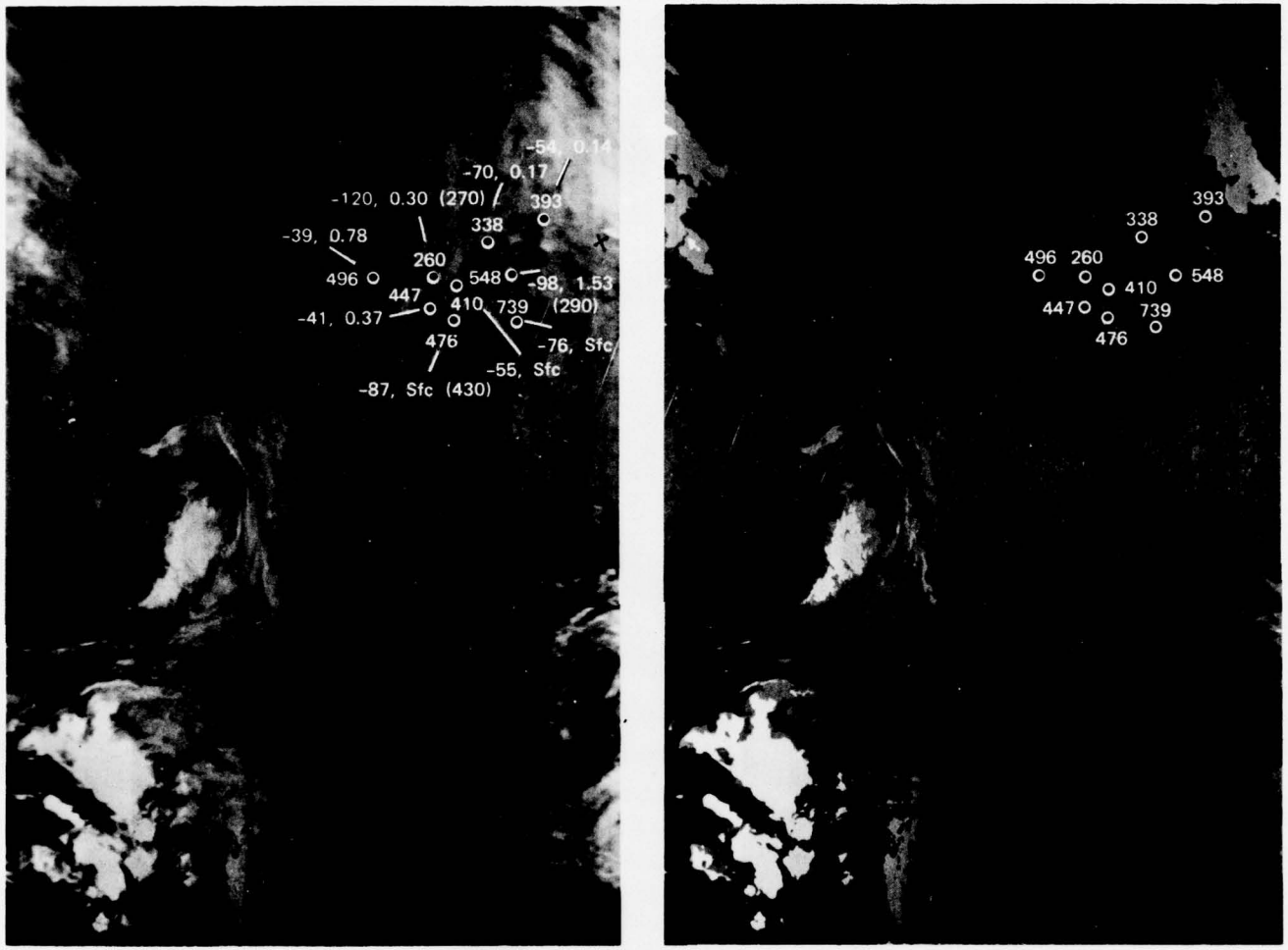

16 GREY SHADE IR

4 GREY SHADE IR

SA-4348-9

FIGURE 9 CLOUD COVER AND REFRACTIVITY GRADIENTS, 19 NOVEMBER 1973

rapidly eastward and at 1200 GMT on the 11th was centered over Rumania. At this time a northeast-southwest cold front was located in the English Channel. This cold front moved through the area of interest on the 11th and 12th.

2. Cloud Cover

At the start of the period, there were scattered low clouds over the area of interest. At 0000 GMT on the 10th the area was clear. Subsequently, a well defined frontal band with multiple layers of clouds moved through the area. Behind the frontal band there was a broken to overcast layer of stratus and stratocumulus.

3. Refractivity Gradients

Rawinsonde soundings taken at eight different times were examined for this case study. Figure 10 shows the distribution of layers with superrefractive gradients (and one layer with a trapping gradient) during the period studied. None of the stations had layers with superrefractive gradients throughout the entire period. Two stations, 447 and 548, had no layers with superrefractive or trapping gradients during the period studied. The largest number of stations simultaneously having layers with superrefractive gradients was five (at 1200 GMT on the 11th), and these stations were widely scattered, with stations in between them having no superrefractive gradients. Only one of the layers with gradients of superrefractive magnitude in this case was surface based (station 496). The remainder were at various altitudes up to 2.55 km (station 410).

Figures 11 and 12 show cloud cover and refractivity gradients for two selected times during the period. Figure 11 (at 0010 GMT on the 7th) shows a diffuse frontal band extending northeast-southwest across northern Italy. There are some cellular clouds just east of the British Isles, and between these cells and the band there are scattered low and

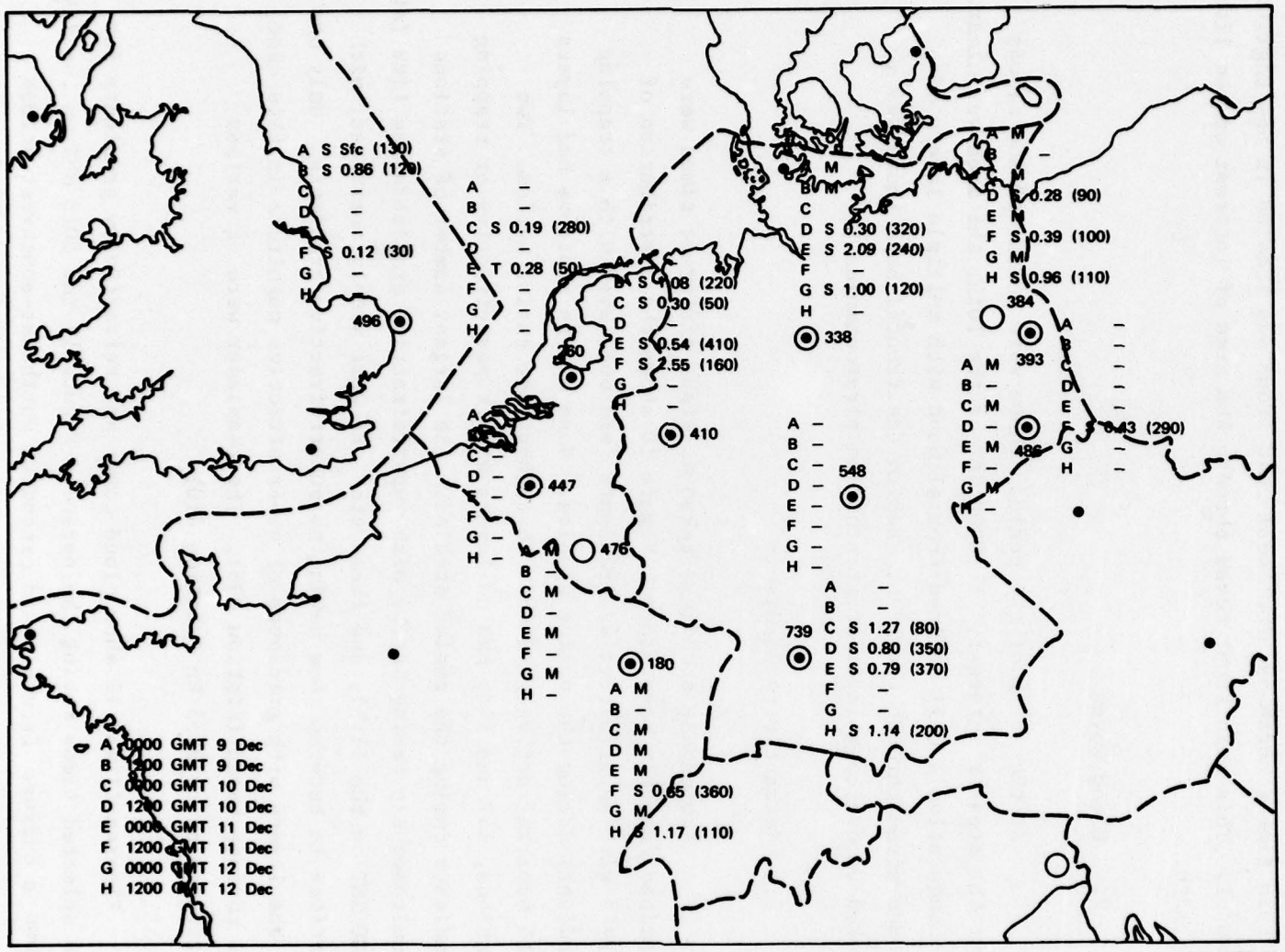

FIGURE 10 HEIGHT OF BASE (KM) AND THICKNESS (METERS) OF LAYERS WITH SUPERREFRACTIVE (S) OR TRAPPING (T) N-GRADIENTS 9 TO 12 DECEMBER 1973

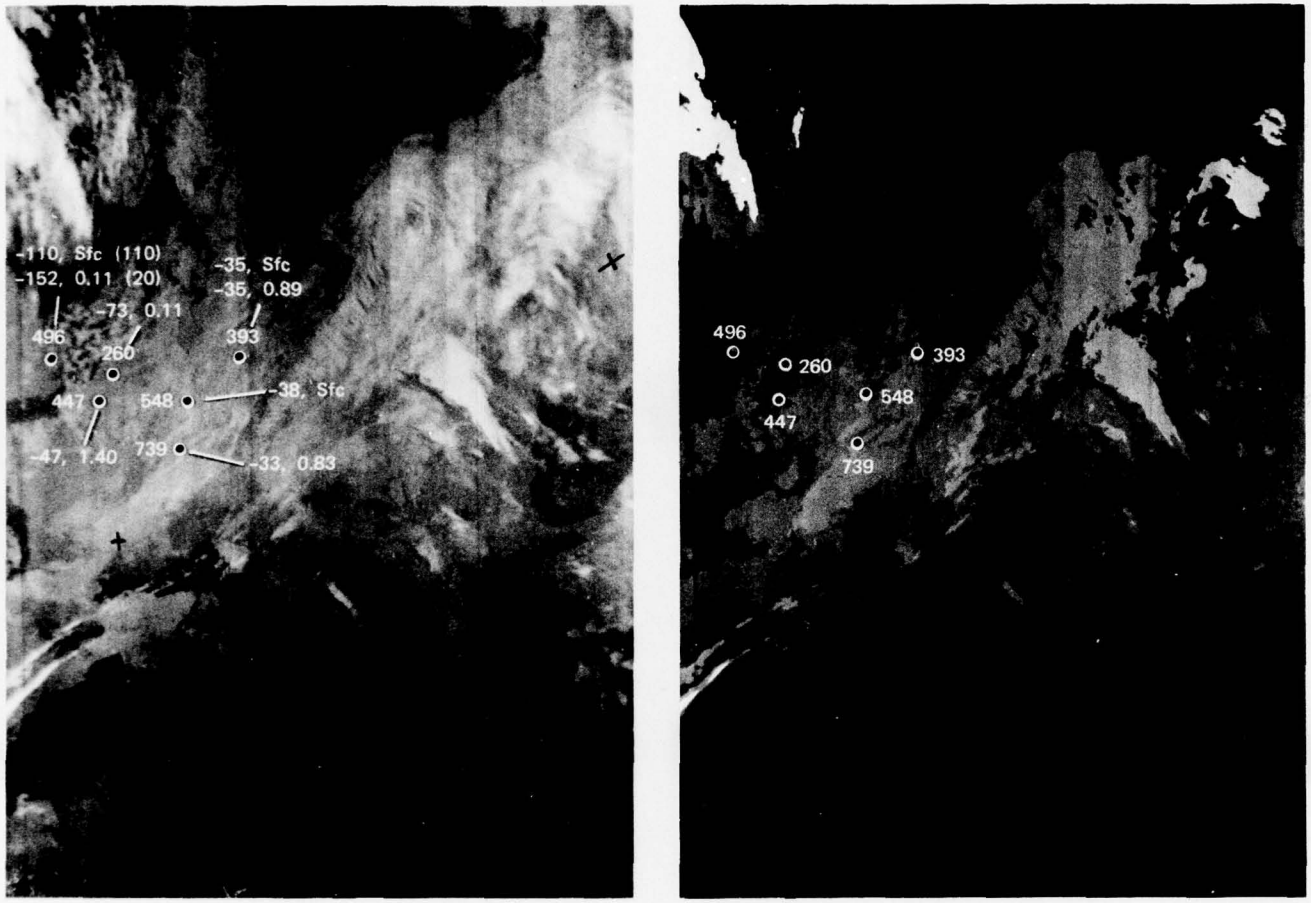

SA-4348-11

16 GREY SHADE IR

4 GREY SHADE IR

FIGURE 11 CLOUD COVER AND REFRACTIVITY GRADIENTS, 9 DECEMBER 1973

middle clouds. Refractivity gradients on the overlay (measured at 0000 GMT on the 9th) decrease in magnitude from southeast to northwest with a surface based layer with superrefractive gradients at station 496 (where the cellular clouds are located). The largest negative refractivity gradients at the other stations are located at various altitudes between the surface and 1.4 km. The cloud cover over the three stations to the east appears (in the four grey shade IR photograph) to consist of low and middle clouds. At stations 260 and 447 where the refractivity gradients are more negative, it appears to be clear.

Figure 12 shows the cloud cover at 2037 GMT on the 11th and refractivity gradients at 0000 GMT on the 12th. To compensate for this time difference, the plotted locations of the gradients have been placed so that they are in the proper position with respect to the band and thus are not in the correct geographical location. Only one refractivity gradient (-80 N-units/km at station 338) is close to superrefractive magnitude. This is consistent with the results of Blackmer (1974) who found that lower received signal levels (indicative of the absence of superrefraction) on a tropospheric scatter link were more frequent behind a frontal band.

Comparison of cloud photographs and refractivity gradients at other times during this case study showed considerable variability in the height and magnitude of refractivity gradients. The largest negative refractivity gradients were in clear areas or areas of low cloud ahead of the frontal band. One gradient of -98 N-units/km was, however, found near the center of the band.

F. 0000 GMT 20 January to 1200 GMT 22 January 1974

1. Synoptic Situation

Early in the period, a high pressure area with a central pressure of 1040 mb was centered over northwestern France. This high

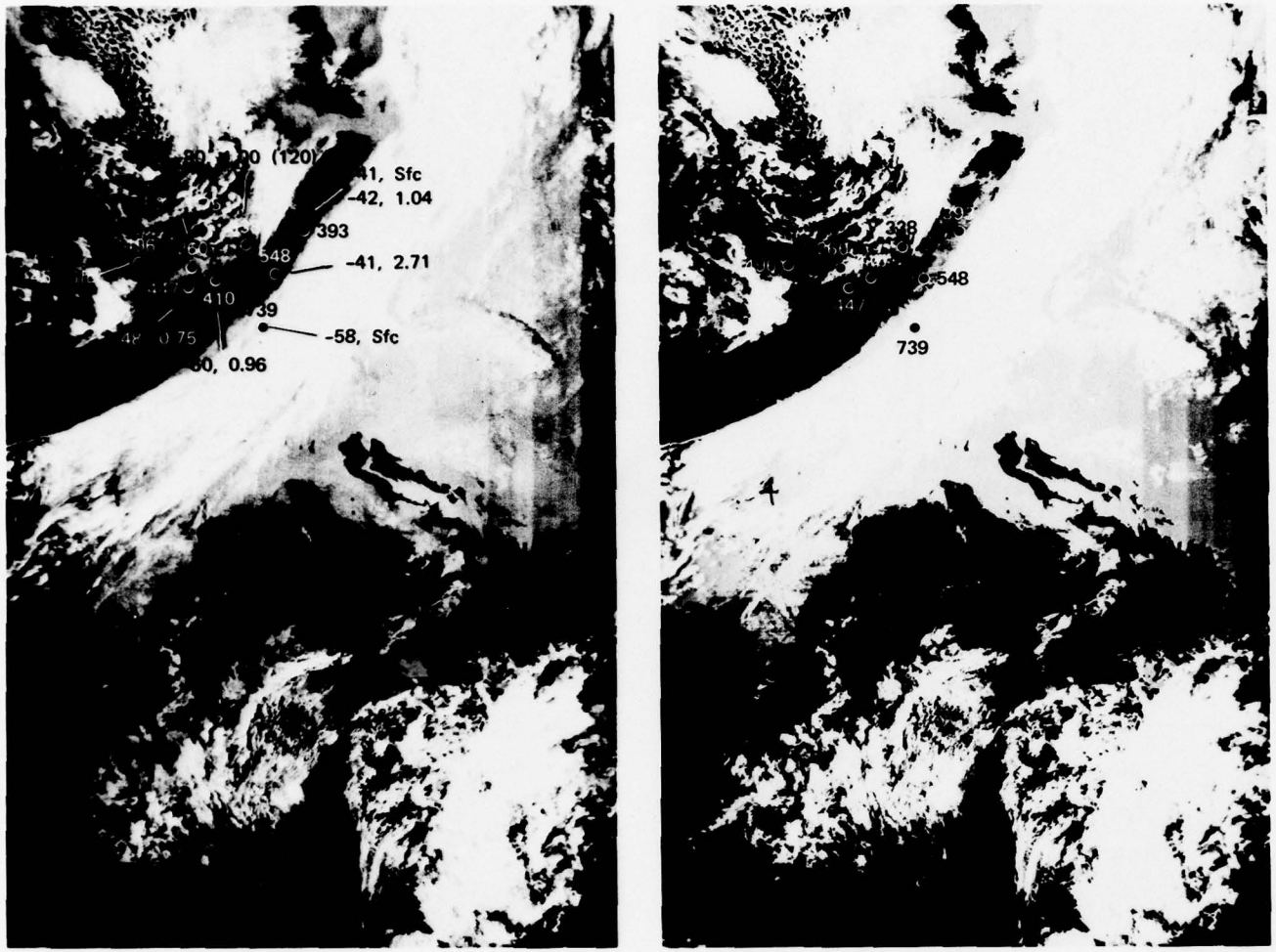

16 GREY SHADE IR

4 GREY SHADE IR

FIGURE 12 CLOUD COVER AND REFRACTIVITY GRADIENTS, 11 DECEMBER 1973

pressure area gradually moved eastward and the pressure at the center decreased. By the 22nd, there was an elongated ridge of high pressure with several minor centers extending east-northeastward across western Europe. This condition prevailed on the 23rd while on the 24th a cold front moved into western Europe from the northwest.

2. Cloud Cover

An extensive blanket of fog and low stratiform clouds covered the majority of the area throughout the period. This fog reduced horizontal visibility at the surface to less than a kilometer at a number of stations.

3. Refractivity Gradients

A number of large negative refractivity gradients were computed from rawinsonde data for this case study. These large gradients were the result of a strong (typically 10 to 15°C) temperature inversion and a large (25 to 30°C) decrease in dew point depression. The height of the base of the inversion fluctuated but was generally within plus or minus 50 mb of the 900 mb level.

Figure 13 shows the base and thickness of layers with superrefractive and trapping gradients at the various stations during the period studied. The figure shows that four stations (496, 260, 410, and 338) had layers with superrefractive or trapping gradients at all six times examined. Even stations 447 and 548 had superrefractive gradients at three of the six times examined. At two times (1200 GMT 20 and 21 January) the layer with superrefractive or trapping gradients was simultaneously observed by all but one or two stations at the eastern edge of the station network. With two exceptions, the layer (two layers at station 338) was not based at the surface but at altitudes ranging from less than 0.5 to greater than 2 km.

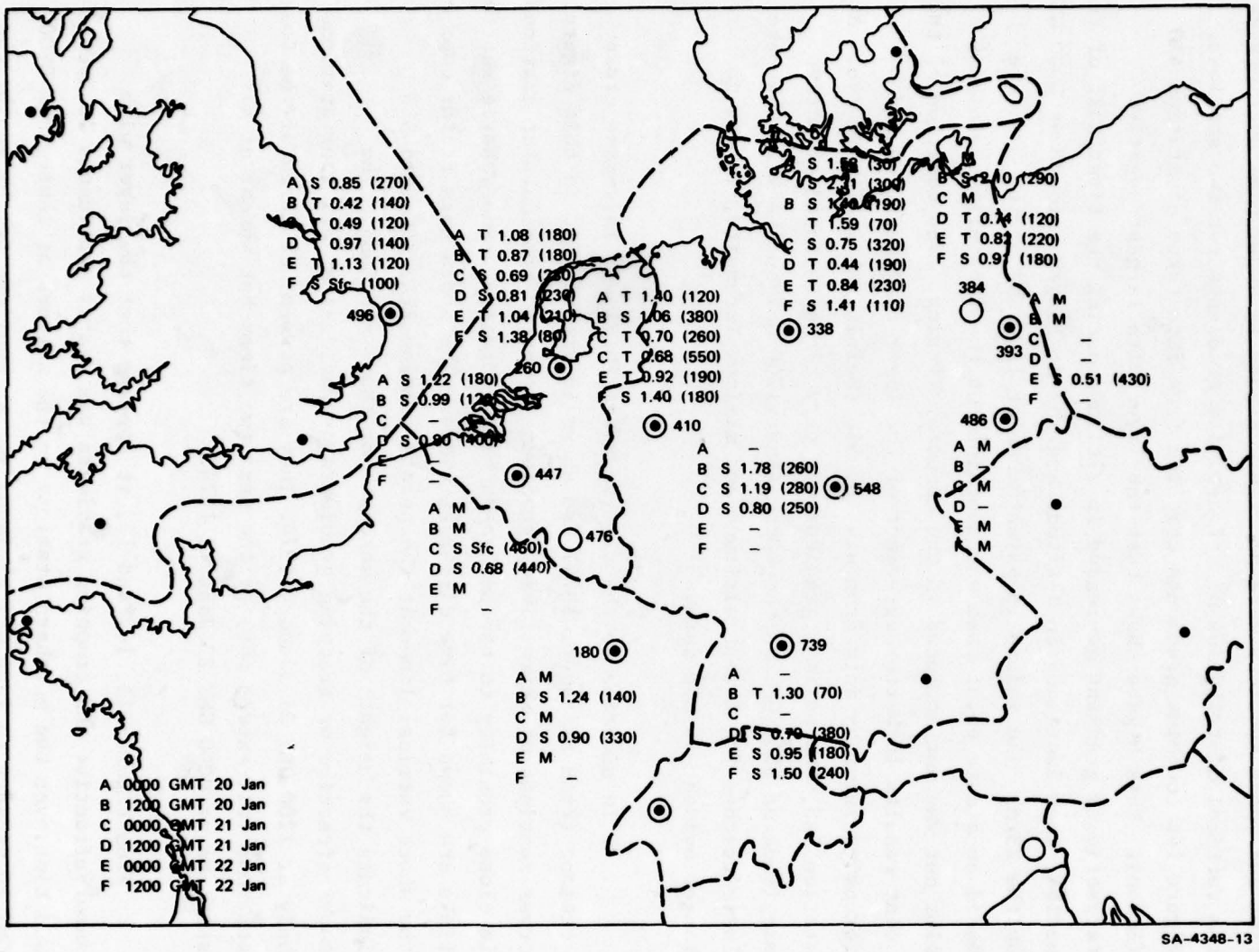

FIGURE 13 HEIGHT OF BASE (KM) AND THICKNESS (METERS) OF LAYERS WITH SUPERREFRACTIVE (S) OR TRAPPING (T) N-GRADIENTS 20 TO 22 JANUARY 1974

Since the layer was nearly continuous over the area, selected time and space sections were plotted. Figure 14 shows time sections of the vertical distribution of refractivity gradients for two stations. Figure 14a contains gradients computed from data taken at station 410 (Essen). This figure shows that the layer with largest negative refractivity gradient decreased in altitude during the first half of the period, then increased in altitude and was no longer evident at 0000 GMT on the 23rd. The values in parentheses at 1200 GMT on the 21st are based on a data point that was contained on the facsimile rawinsonde plot but was not included in the computer listing. The addition of this point results in better agreement of the layer configuration and intensity shown by data from station 548 (Meiningen) in Figure 14b. At station 548, the maximum gradient was very close to superrefractive magnitude at 0000 GMT on the 20th. After 1200 GMT on the 21st when the layer reached its lowest altitude and maximum intensity, it was no longer evident in the data.

In addition to the time sections in Figure 14, space cross sections (from Blackmer, 1974) are shown in Figure 15. In this figure cross sections of refractivity gradients computed from data at stations in close proximity to the Berlin-Bocksberg-Breitsol tropospheric scatter links are shown for five different times. The cross bars at the tops of the short vertical lines at the points labeled BTL, BBG, and BLN indicate the heights of the antennae at those stations. The superrefractive or trapping gradients are evident at all four stations only at 1200 GMT 21 January 1974. They are present at three of the four stations (all except 548) at the next two times but absent at all stations at 0000 GMT 23 January 1974.

From Figures 13, 14, and 15, it appears that the layer with superrefractive and trapping gradients was nearly continuous in space and time over the northern stations in the network at least from 0000 GMT 20 Janaury to 1200 GMT 22 January. At stations to the south, the layer was not continuous. All stations on Figure 13 show the decrease in

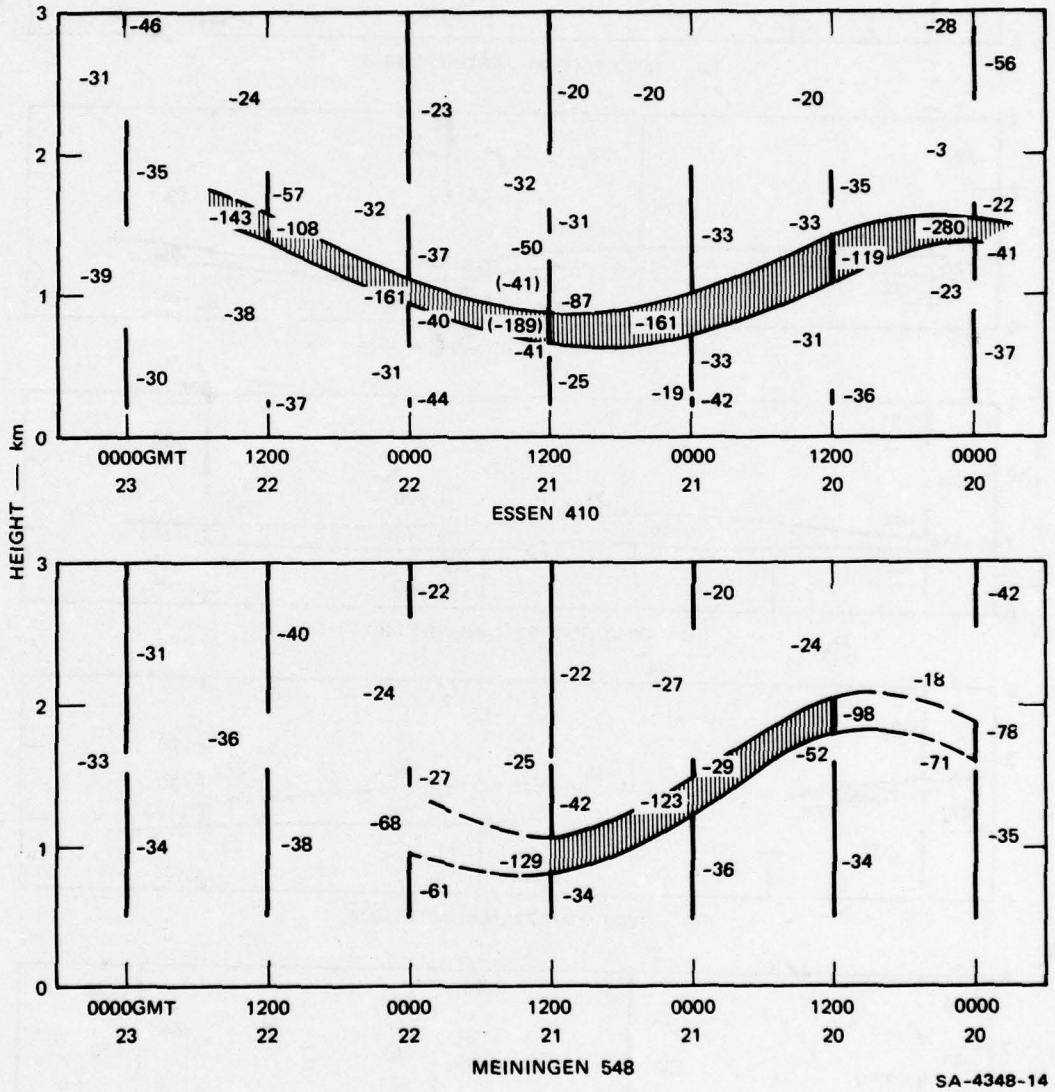

FIGURE 14 TIME SECTIONS OF REFRACTIVITY GRADIENTS (N-UNITS/KM) AT ESSEN AND MEININGEN 20 TO 23 JANUARY 1974

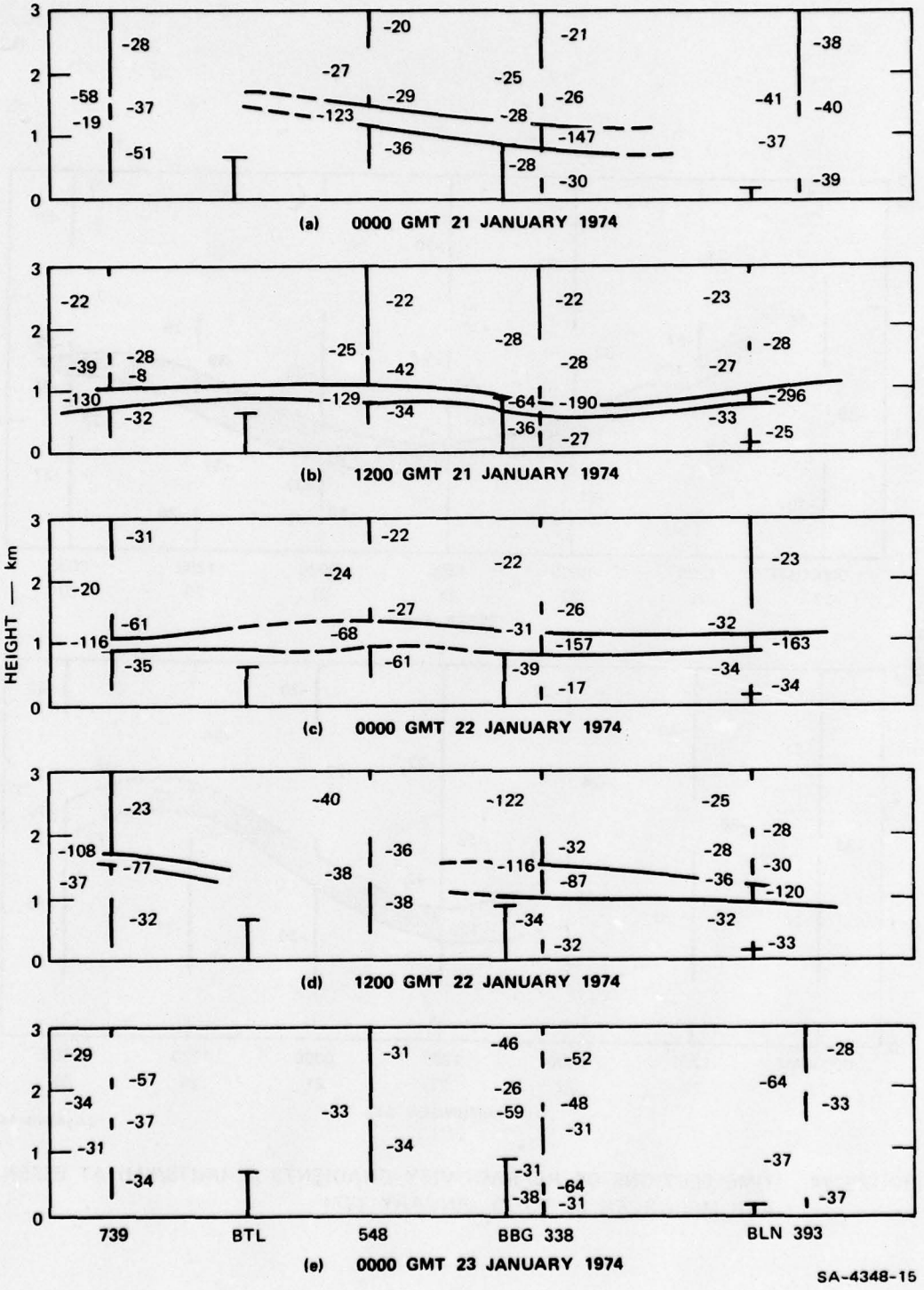

FIGURE 15 CROSS SECTIONS OF REFRACTIVITY GRADIENTS (N-UNITS/KM) ALONG THE BREITSOL (BTL) BOCKSBERG (BBG) BERLIN (BLN) TROPOSPHERIC SCATTER LINKS, 21 TO 23 JANUARY 1974

height of the layer during the middle of the period, as was shown by the time sections for stations 410 and 548 in Figure 14.

Figures 16 and 17 show cloud cover and refractivity gradients for two times during the period. Temperatures at the base of the inversion are entered on the right half of the overlay. The cloud cover in Figure 16 was photographed at 2037 GMT on the 19th while the refractivity gradients are from data taken at 0000 GMT on the 20th. Because of the general continuity in space and time of the layer of superrefractive or trapping gradients the 3 1/2 hour time difference is not considered significant. The left photograph in Figure 16 shows a featureless grey background in the area of the rawinsonde stations. This is typical of fog and low stratus. The photograph on the right shows that the stations are in an area of warmest temperatures (blackest grey shades). In this case the temperature of the blackest grey shade is greater than $0^{o}C$. The temperatures at the base of the inversion (on the right of the overlay) are $0^{o}C$ or warmer at the three northerly stations and slightly colder than $0^{o}C$ at the three southerly stations. Examination of refractivity gradients on the left of the overlay show that all stations except 548 have superrefractive or trapping gradients. The height of the base of the layer (except at station 496) is above 1 km.

The cloud cover on the left of Figure 17 (photographed at 2142 GMT on the 21st again shows a rather uniform grey background in the area of the rawinsonde stations. The right hand photograph, however, shows that most of the stations are in an area of light grey which corresponds to a temperature range of 0 to $-10^{o}C$. The temperatures (shown on the right of the overlay) at the base on the inversion are all colder than $0^{o}C$. The warmest temperature is at station 548 which is in the darkest area on the cloud photograph. The maximum negative refractivity gradients (shown on the left of the overlay) generally have bases below 1 km. Many of the gradients at this time are of trapping magnitude while on the Figure 16 overlay, only one gradient greatly exceeded the $\leq$ -157 N-units/km trapping criteria. There were not enough of the four grey

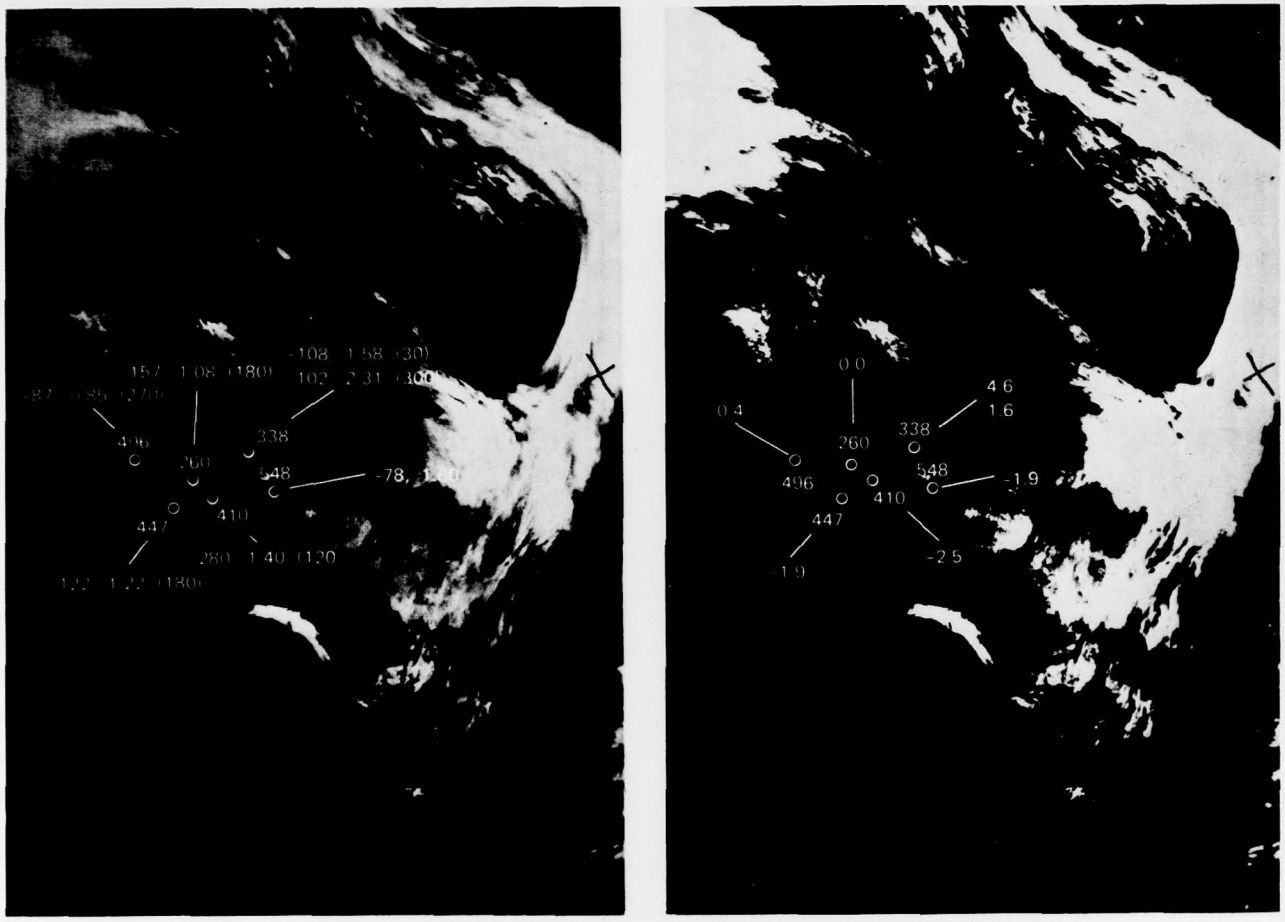

SA-4348-16

16 GREY SHADE IR

4 GREY SHADE IR

FIGURE 16 CLOUD COVER AND REFRACTIVITY GRADIENTS, 19 JANUARY 1974

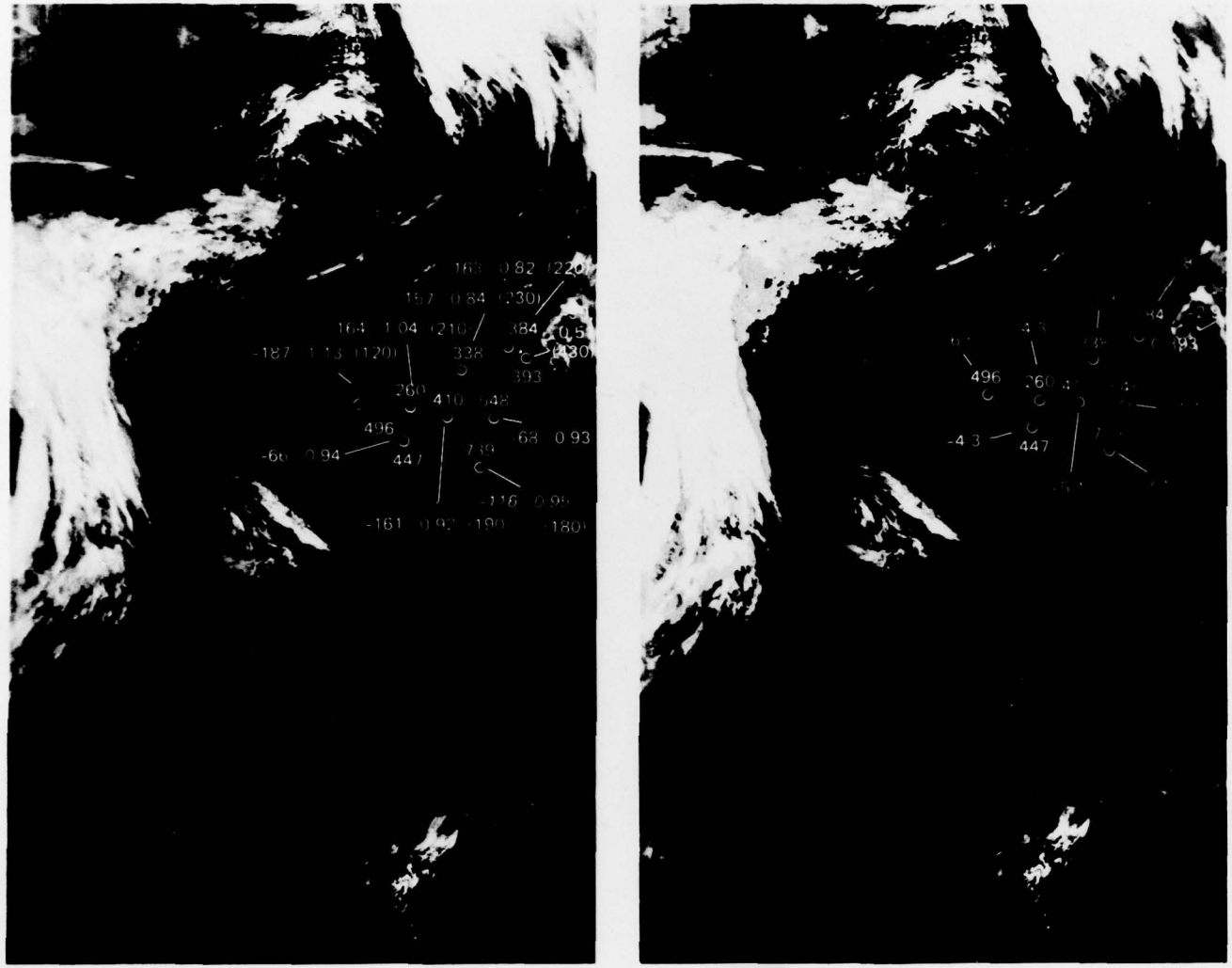

16 GREY SHADE IR

4 GREY SHADE IR

SA-4348-17

FIGURE 17 CLOUD COVER AND REFRACTIVITY GRADIENTS, 21 JANUARY 1974

shade IR photographs at times close to rawinsonde observation time to determine whether there was any significance in the apparent height of the fog and cloud layer top and the height and magnitude of the refractive gradients.

G. 0000 GMT 12 February to 1200 GMT 17 February 1974

1. Synoptic Situation

At the start of this period, a large deep low pressure area was located between Scotland and Ireland. This low pressure area expanded and had three centers at 0000 GMT on the 13th. At that time, a migratory cyclone was developing in the western Atlantic. This migratory cyclone moved eastward and by 1200 GMT on the 15th was located over Ireland with two 970 mb centers. It remained in this vicinity for the next 24 hours and the central pressure increased to 1000 mb. Several frontal systems associated with the low pressure areas moved through western Europe during this period.

2. Cloud Cover

Extensive cloud cover was associated with the low pressure area at the start of the period. Much of the area was only partly covered by low and middle clouds following the passage of the frontal system. The next frontal system brought extensive cloud cover into the area on the 15th. Behind this front, there were scattered small areas of fog and low stratiform clouds.

3. Refractivity Gradients

Large negative refractivity gradients were evident only in data from one station on the 12th and one station on the 13th. The largest negative gradient at 0000 GMT on the 14th was only -54N-units/km. Subsequently, gradients of superrefractive magnitude were more

numerous. Figure 18 shows the distribution of gradients of superrefractive magnitude from 1200 GMT 14 February to 1200 GMT 17 February 1974. The figure shows that the occurrence of superrefraction was most frequent at stations 338 and 384 and no superrefractive gradients were computed from data taken at stations 260, 548, and 393. Superrefractive gradients were computed from data from four stations both at 0000 GMT on the 15th and at 1200 GMT on the 16th. At both times, both surface based layers with superrefractive gradients and layers with superrefractive gradients aloft were noted. Figures 19 and 20 are cloud photographs with overlays showing the distribution of refractivity gradients at the two times mentioned above. The cloud photographs at 0035 GMT on the 15th (Figure 19) show that a number of the stations are in a clear area ahead of a frontal band. Two of the stations (338 and 739) have a surface based layer with superrefractive gradients, and stations (410 and 476) (closer to the band) have a layer with superrefractive gradients near the 1.5 km level. Station 496 beneath the band (from which heavy precipitation is falling) has a maximum gradient of -46 N-units/km based at the surface. Station 548 in the clear area has a gradient only 1 N-unit/km less, also based at the surface.

Figure 20 shows cloud cover at 1122 GMT 16 February and the overlay on the figure shows refractivity gradients computed from data at 1200 GMT on the 16th. A major feature of the cloud cover shown by the photographs is the remnants of the frontal band. There are patches of cloud at various altitudes and an area of fog (to the southeast of station 739). Refractivity gradients of superrefractive magnitude appear at four of the stations. At station 496 furthest to the northwest, where the cloud cover is a mixture of very low (warm on the four grey shade IR photographs) stratus and stratocumulus, the layer with superrefractive gradients is based at the surface. At the other three stations, where the cloud cover is mostly middle and high clouds, (as shown by the colder temperatures on the four grey shade IR

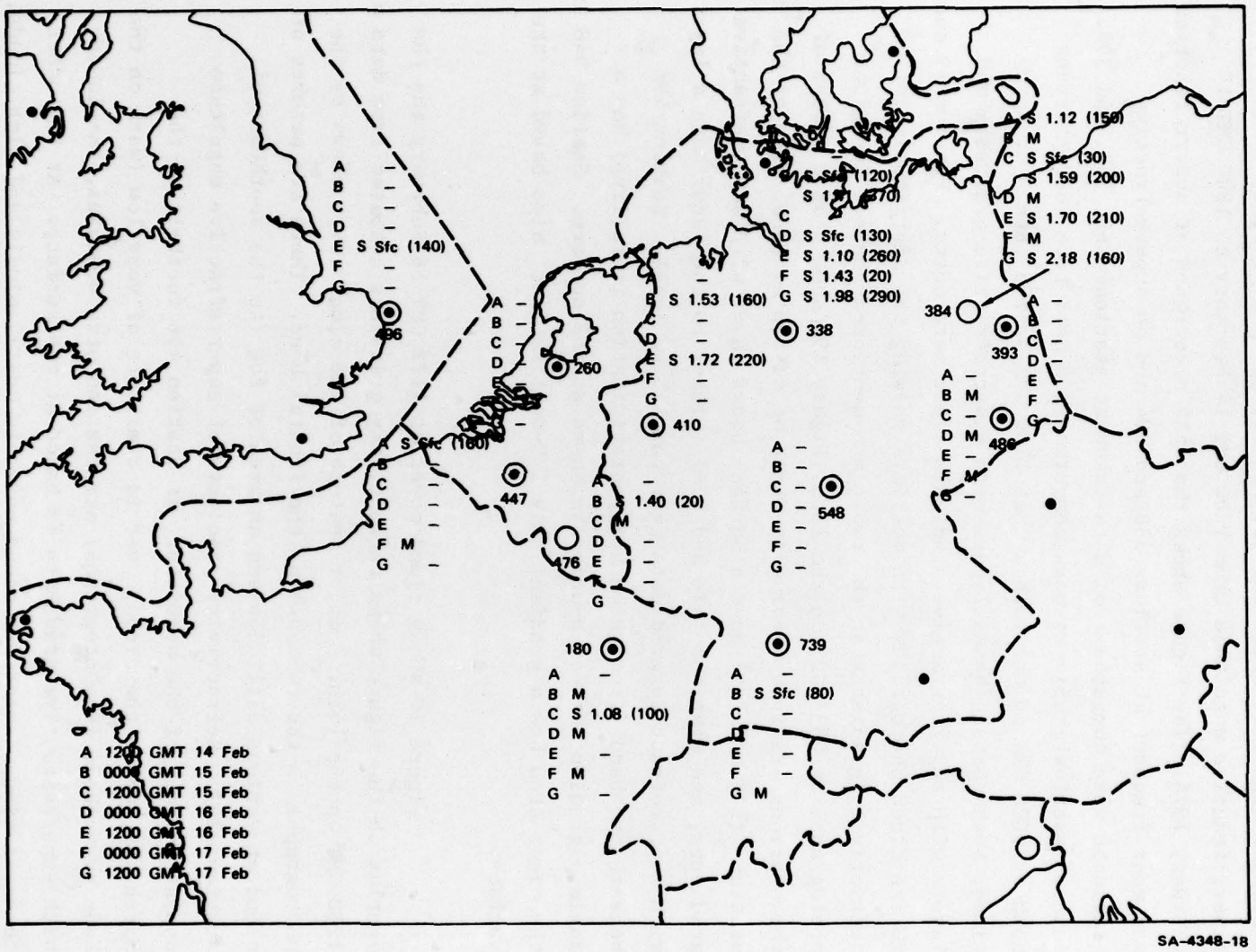

FIGURE 18 HEIGHT OF BASE (KM) AND THICKNESS (METERS) OF LAYERS WITH SUPERREFRACTIVE (S) OR TRAPPING (T) N-GRADIENTS 14 TO 17 FEBRUARY 1974

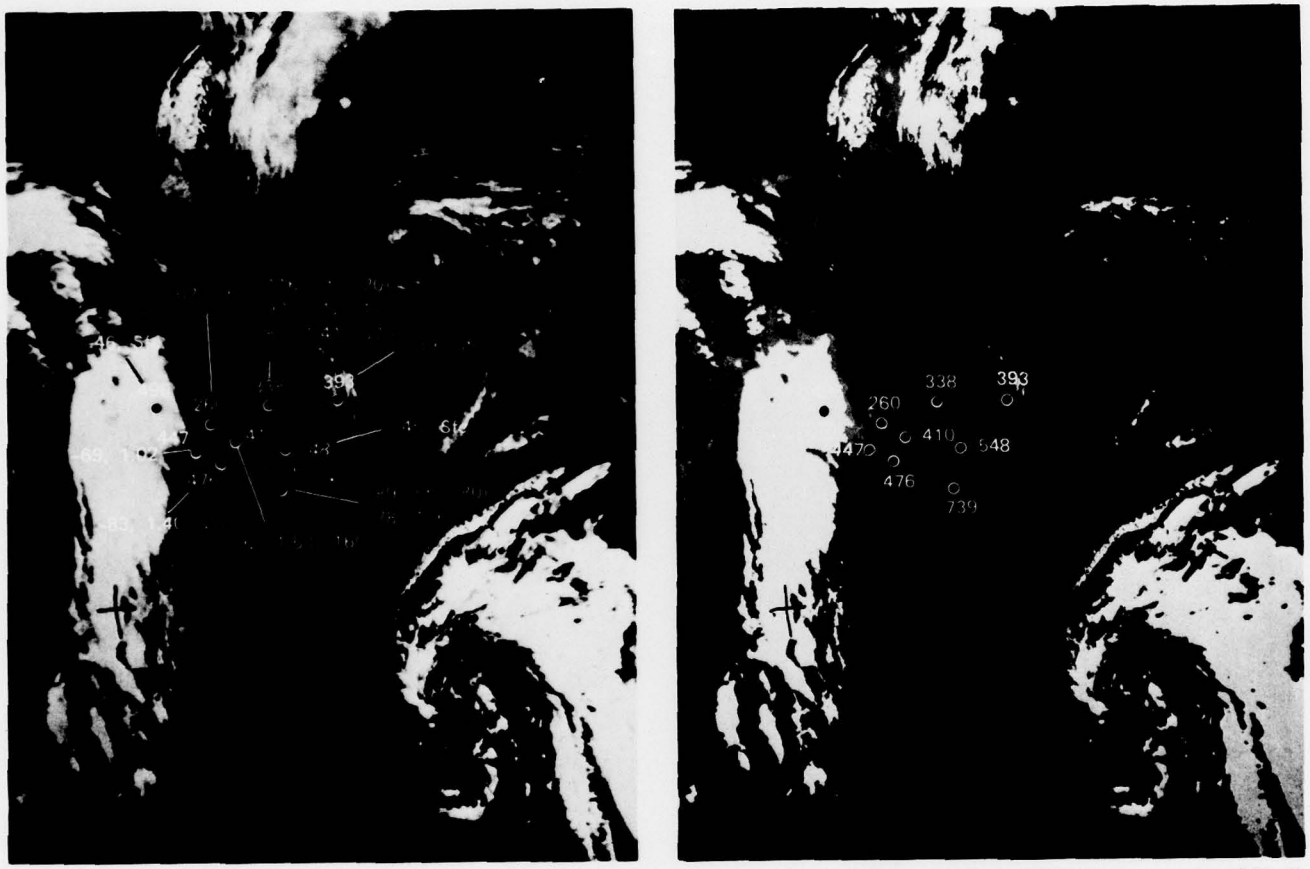

SA-4348-19

16 GREY SHADE IR

4 GREY SHADE IR

FIGURE 19 CLOUD COVER AND REFRACTIVITY GRADIENTS, 15 FEBRUARY 1974

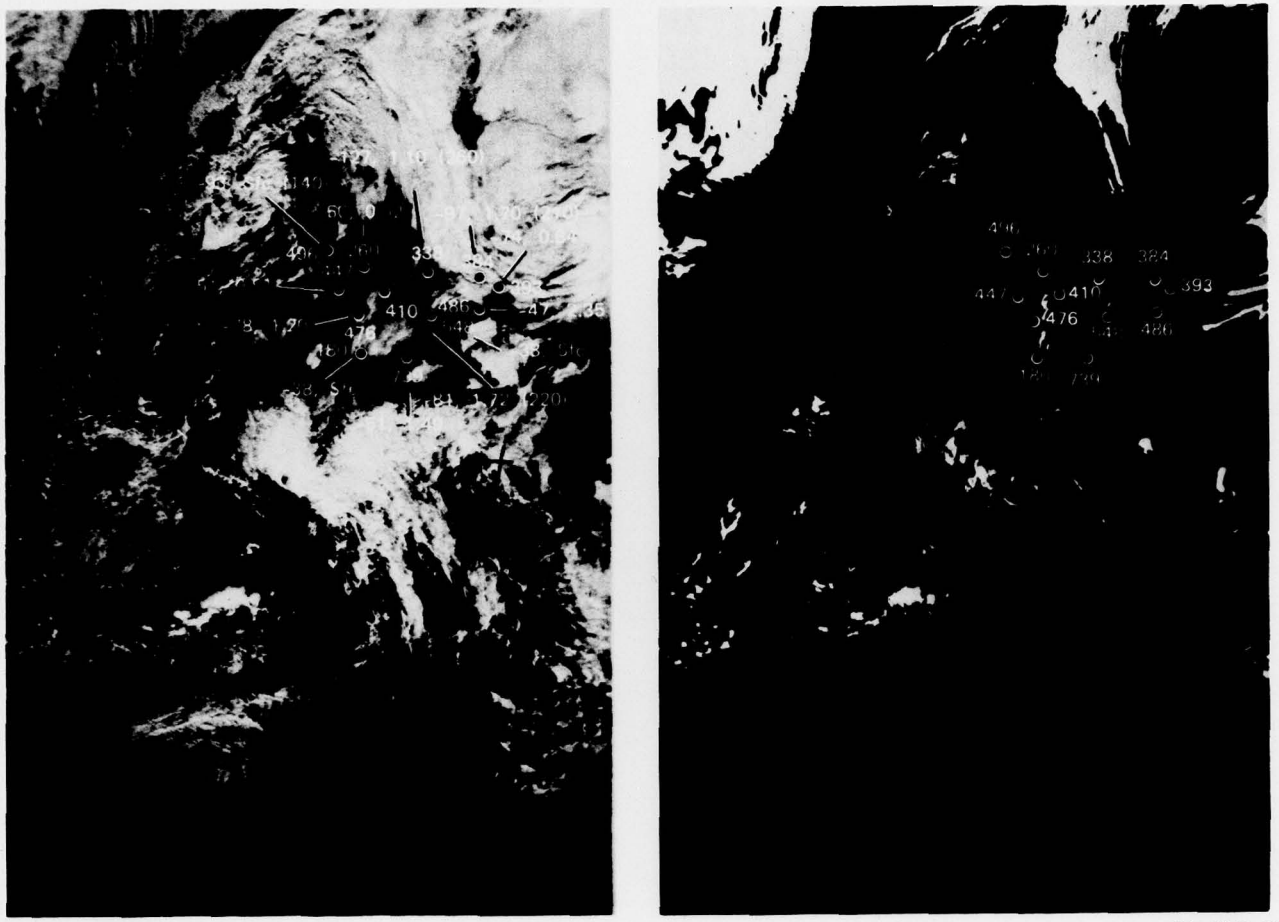

SA-4348-20

1/3-MILE VISIBLE

4 GREY SHADE IR

FIGURE 20 CLOUD COVER AND REFRACTIVITY GRADIENTS, 16 FEBRUARY 1974

photograph) the base of the layer with superrefractive gradients is above 1 km. In this example (and from comparisons of cloud layers and refractivity gradients at other times in this case study) there was considerable variability between adjacent stations in the distribution (height and magnitude) of refractivity gradients even though the cloud cover or its absence appeared to be the same over adjacent stations. The largest negative refractivity gradients, however, appeared to occur in clear areas or in areas of broken clouds.

IV DISCUSSION OF RESULTS

In the cases studied there was considerable variability in magnitude and height of the largest negative refractivity gradients. All cases, however, had some refractivity gradients of superrefractive or trapping magnitude and these were generally located in clear areas or areas of scattered or broken clouds. This is in agreement with the results of Blackmer (1974) who found generally higher signal levels on the Berlin-Bocksberg-Bristol tropospheric scatter communication links associated with either clear conditions or low clouds.

In the case study with the best agreement between the cloud cover and distribution of refractivity gradients of superrefractive or trapping magnitude, there was a strong low level inversion and the top of the low cloud and fog layer coincided with the inversion layer. Nearly all the stations within this area of fog and low clouds simultaneously had refractivity gradients of superrefractive or trapping magnitudes at comparable heights at a given time.

Cloud cover was not as uniform over the rawinsonde network during the other five cases studied but even in those situations where cloud cover (or its absence) appeared similar over adjacent stations refractivity gradients computed from data at adjacent stations were often quite dissimilar. In situations where there is no cloud cover over a large area, one would expect that local terrain features would give rise to differences in rawinsonde soundings in the lowest layers of the atmosphere. At higher altitudes, where the effects of the surface should be less one would expect considerable similarity between rawinsonde soundings at stations in close proximity to one another. This expected similarity was not found in many instances in this study. There are two possibilities for the differences between adjacent

stations. First, there is the possibility that in a large clear area the temperature and moisture structure of the atmosphere varies considerably over short distances. If this were true, it would be expected that these variations would be observed at one station at one time and at another station at another time. This was not the case, and hence, a second possibility must be considered. This second possibility is that there were differences in the analysis of the original rawinsonde data by the personnel at different stations. This possibility can be investigated by a comparison of the frequency of superrefractive and trapping gradients at the various stations. Table 1 lists the number of rawinsonde ascents (raobs) examined from the various stations, the number of superrefractive or trapping gradients computed from the data (some stations had more than one large negative gradient) at a given time, and the number and percent of the rawinsonde ascents that contained no superrefractive or trapping gradients. The table shows that three of the stations (548, 447, and 393) have a very large percent of rawinsondes with no superrefractive or trapping gradients. The number of surface based layers with superrefractive or trapping gradients at these three stations is roughly comparable to that at the others; the major difference is in the frequency of layers aloft.

A possible reason for the absence of large negative refractivity gradients at some stations can be found by comparing the number of data points (between the surface and the 700-mb level) in rawinsonde ascents from a station with many superrefractive and trapping gradients with the number of data points from a station with few such gradients. Table 2 makes such a comparison using data from stations 410 and 548. The table shows that station 410 consistently reported more levels than station 548; the averages for the two stations are about nine and six points per sounding. A difference of about one data point per sounding may be accounted for by the fact that station 548 is at an elevation (1/2 km) where the surface pressure is less than 1000 mb so that this mandatory level cannot be included. During the February period, low surface pressure in the area resulted in the absence of this level in the data

Table 1

FREQUENCY OF SUPERREFRACTIVE OR TRAPPING GRADIENTS AT VARIOUS STATIONS

Station	No. Raobs	No. of Superrefractive or Trapping Gradients		
		Surface	Aloft	None (%of Raobs)
260	35	3	17	15 (42.9)
410	35	4	21	14 (40.0)
548	35	2	4	29 (82.9)
496	34	7	15	13 (38.2)
739	34	4	15	17 (50.0)
338	33	6	22	10 (30.3)
447	33	2	3	28 (84.8)
393	32	1	3	28 (87.5)
476	27	4	8	16 (59.3)
384	20	1	18	4 (20.0)

Table 2

COMPARISON OF NUMBER OF DATA POINTS IN RAWINSONDE ASCENTS AT TWO STATIONS DURING PERIODS STUDIED

Period	Stations		Number of Raobs
	410	548	
1, 2 October	33	19	3
5-7 October	48	36	5
18-20 November	50	33	6
9-12 December	75	52	8
20-22 January	50	35	6
14-17 February	56	41	7
Total	312	216	35
Average	8.91	6.17	

from station 410. The least number of data points in a rawinsonde from station 548 was three. There were the surface, 850, and 700-mb levels. There were four soundings with four data points and only one with nine data points. The maximum and minimum number of points in a sounding from station 548 were 13 and 6, respectively. This maximum was observed on two occasions, and on these occasions the largest negative refractivity gradients were -75 and -80 N-units/km. These gradients illustrate the fact that a large number of data points do not always result in large refractivity gradients and vice versa. For example, in a sounding with seven data points (station 338 at 1200 GMT 6 October), three superrefractive gradients and one trapping gradient were computed. It is obvious, however, that the probability of detecting a superrefractive or trapping gradient increases as the number of data points in the sounding increases. For this reason, it is concluded that the fewer data points in the soundings from station 548 result in fewer computed superrefractive and trapping gradients at that station. The opposite viewpoint is rejected--that is, that the atmospheric structure is consistently less complicated at station 548 than at station 410 and therefore can be described by fewer data points.

In many instances, the layers with superrefractive or trapping gradients resulted from very small discontinuities in the temperature and moisture while the larger scale discontinuities, with which the clouds are more likely to be associated, were not large enough to give refractivity gradients of superrefractive or trapping magnitudes.

V CONCLUSIONS

This brief study of how well the type and variability of satellite-viewed cloud cover may be used to describe the occurrence and variability of anomalous propagation conditions over areas of various sizes showed that except in one of the six cases studied, refractivity gradients varied markedly between adjacent stations that appeared to have similar cloud cover. The reason for this variability appears to stem from the fact that some of the stations did not describe the atmospheric structure in sufficient detail for large negative refractivity gradients to be detected. That is, three of the stations in the rawinsonde network had no superrefractive or trapping gradients in over 80 percent of the rawinsondes, while the other stations had such gradients in 50 to 80 percent of the rawinsondes. It does not seem likely that the atmospheric structure would consistently be less complicated at three of the stations. Therefore, the absence of superrefractive or trapping gradients at these three stations is believed to be due to the manner in which the original rawinsonde data were analyzed at the station.

Because of these inconsistencies in the rawinsonde data it was not possible to make an adequate assessment of the use of satellite-viewed cloud cover for indicating the occurrence of anomalous propagation conditions.

The postulate that satellite-viewed cloud cover may be a valuable aid in indicating potential areas of anomalous propagation is, however, not precluded by the results of the study. For example, cloud cover in the six cases studied varied from extensive clear areas to a very extensive area of fog and low stratus. There were no cases where there was

widespread multilevel cloud cover with associated refractivity gradients of superrefractive or trapping magnitudes. This correspondence of large negative refractivity gradients with either clear conditions or predominantly low clouds is in agreement with the results of Blackmer (1974) who found generally higher received signal levels or the Berlin-Bocksberg Breitsol tropospheric scatter communication links with these classes of cloud cover.

The unique case in which the data from all reliable rawinsonde stations showed refractivity gradients of superrefractive or trapping magnitudes was one where the satellite photographs showed a very extensive area of fog and low clouds. In this case the satellite-observed cloud cover could be used to infer the presence of similar large negative refractivity gradients and anomalous propagation, throughout the entire area where the satellite photographs showed this clearly characteristic cloud cover.

In view of the importance of the concept of using satellite data for inferring propagation conditions and the limited supporting evidence revealed by the current study, it is recommended that further investigation should be carried out. In such further studies data from a reliable rawinsonde station and visible and IR data from a satellite should be used to construct time sections of cloud cover and refractivity gradients. In the study, distinction should be made between large negative refractivity gradients due to very thin discontinuities in temperature and moisture (which may not be associated with cloud cover) and the less negative gradients occurring with thicker layers of temperature and moisture discontinuities with which the cloud cover is more likely to be associated. These analyses should show the extent to which the height and thickness of layers with various refractivity gradients are associated with major cloud features, or are not correlated with the cloud cover. A study of this type might prove most successful in an area where terrain influence is minimal, such as over the oceans.

REFERENCES

Blackmer, R.H., Jr., 1974: "Cloud Cover Versus Signal Strength Study," Final Report, Contract DAEA18-71-A-0204/0008, SRI Project 2793, Stanford Research Institute, Menlo Park, California.

Blackmer, R.H., Jr., P.A. Davis, and S.M. Serebreny, 1968: "Satellite-Viewed Cloud Cover as a Descriptor of Atmospheric Properties," Final Report, Contract E-126-67(N), SRI Project 6603, Stanford Research Institute, Menlo Park, California.

Blankenship, J.R. and R.A. Savage, 1974: "Electro-Optical Processing of DAPP Meteorological Satellite Data," Bull. Amer. Meteor. Soc., Vol. 55, No. 1, pp. 9-15.

Meyer, W.D., 1973: "Data Acquisition and Processing Program: A Meteorological Data Source," Bull. Amer. Meteor. Soc., Vol. 54, No. 12, pp. 1251-1254.

Serebreny, S.M. and R.H. Blackmer, Jr., 1974: "Satellite-Viewed Cloud Cover as a Descriptor of Tropospheric Radio-Radar Propagation Conditions," Final Report, Contract DAHC04-69-C-0065, SRI Project 7940, Stanford Research Institute, Menlo Park, California.